

# Spin transport through a nanojunction with a precessing anisotropic molecular spin - Gilbert damping and spin-transfer torque

Milena Filipović

*Institute of Physics Belgrade, University of Belgrade, Pregrevica 118, 11080 Belgrade, Serbia*

(Dated: December 10, 2024)

The subject of this study is spin transport through an orbital belonging to a magnetic molecule, connected to two leads, and coupled via exchange interaction with the precessing anisotropic molecular spin in a constant magnetic field. The expressions for spin current components, noise of  $z$ -polarized spin current, spin-transfer torque, Gilbert damping and other torque coefficients are obtained using the Keldysh nonequilibrium Green's functions technique. The precession of the molecular spin, and hence, the inelastic tunnelling processes involving spin-flip events between molecular quasienergy levels, driven by this precession, can be controlled by the uniaxial magnetic anisotropy parameter. By setting the Larmor precession frequency, the tilt angle of molecular magnetization with respect to the magnetic field, and the magnetic anisotropy parameter, one can modulate the spin-current components and noise, spin-transfer torque and related torque coefficients. Moreover, the dc-spin current and spin-transfer torque components provide the quasienergy level structure in the orbital and the torque vanishes for a suppressed molecular spin precession, obtained by proper adjustment of the anisotropy parameter and magnetic field, allowing to reveal the anisotropy parameter via a dc-spin current or torque measurement. The results of the study show that spin transport and spin-transfer torque generated on the anisotropic molecular spin can be manipulated by the uniaxial anisotropy parameter of the molecular spin even in the absence of the magnetic field.

## I. INTRODUCTION

Due to small size and uniaxial magnetic anisotropy which leads to magnetic bistability, single-molecule magnets are potential candidates for magnetic storage and information processing.<sup>1–15</sup> Since energy barrier to molecular spin reversal depends on the magnetic anisotropy parameter,<sup>2,3,16,17</sup> it is important to find ways to control it, e.g., via charge current or electric field.<sup>8–10,18–24</sup> For the potential applications in spintronics, various phenomena in magnetic structures have been subject of research, such as spin relaxation,<sup>25–29</sup> spin fluctuations,<sup>30–32</sup> geometrical spin torque,<sup>33,34</sup> self-induced torque<sup>35</sup> and dynamics of magnetization driven by external means.<sup>36–48</sup> The control of magnetization in junctions by spin-polarized current was first theoretically suggested<sup>49,50</sup> and then experimentally confirmed.<sup>51,52</sup> By applying spin torque, the magnetization dynamics can be manipulated,<sup>49</sup> and as a back action the spin pumping occurs.<sup>53,54</sup> It is possible to reverse magnetization via current-induced spin-transfer torque.<sup>36,55–60</sup> For instance, using spin-polarized current through a single molecule magnet connected with ferromagnetic electrodes, its spin states can be switched.<sup>17,61–64</sup> It has been shown that the anisotropic molecular spin can be reversed even in the absence of a magnetic field by tuning on a bias voltage for one ferromagnetic and one paramagnetic lead.<sup>65</sup> Spin-polarized currents exert spin-transfer torques on the magnetization of the magnetic nanostructures in the form of field-like torques or damping torques.<sup>36,66–72</sup> The effect of superconductivity on the magnetization dynamics has also been studied since the beginning of the new century.<sup>44,73–79</sup>

The nonequilibrium Green's functions (NEGF) formalism<sup>80–82</sup> has been employed in molecular spintron-

ics in investigations of e.g., spin pumps,<sup>83,84</sup> quantum interference,<sup>85</sup> spin-flip inelastic tunnelling,<sup>86–89</sup> and magnetic skyrmion dynamics.<sup>90–92</sup> NEGF technique has also been used in the theoretical calculations of shot noise of spin current.<sup>93–95</sup> While investigating transport through single-molecule magnets, many effects were analysed such as Kondo effect,<sup>96–100</sup> spin-Seebeck effect,<sup>101–103</sup> spin-transfer torque<sup>104,105</sup> and spin blockade.<sup>65,106,107</sup> In molecular spintronics experimental studies of spin polarized currents,<sup>108,109</sup> spin interactions,<sup>110,111</sup> spin valves,<sup>112</sup> and spin-flip inelastic electron tunnelling spectroscopy<sup>8,113</sup> have been done.

The classical magnetization dynamics is usually described by the Landau-Lifshitz-Gilbert (LLG) equation.<sup>114–116</sup> Even thermal effects on the magnetization dynamics have been studied using LLG equation.<sup>117–119</sup> The contribution of spin-transfer torque due to spin-polarized currents can be included in LLG equation,<sup>36,67</sup> and has been derived for molecular magnets,<sup>41,119–121</sup> and various other magnetic systems such as spin-valves or magnetic multilayers,<sup>49</sup> magnetic domain walls,<sup>122</sup> for slowly varying magnetization,<sup>123</sup> and magnetic skyrmions.<sup>92,124</sup> In quantum transport calculations, the semiclassical approach is often used, where the local magnetization of a magnetic nanostructure is treated as classical and its dynamics is described by LLG equation, while the spin of the conduction electrons is considered as quantum.<sup>34,121,125–130</sup> It is assumed that the spin-polarized currents are carried by electrons that are fast in comparison to the classical, local magnetization dynamics.

The aim of this article is to theoretically study the spin transport through a single molecular orbital of a molecular magnet with a precessing anisotropic spin in a constant magnetic field. The precession frequency of

the molecular spin involves Larmor precession frequency and a term with the uniaxial magnetic anisotropy parameter. The spin in the orbital and molecular spin are coupled via exchange interaction. The orbital is connected to two normal metal leads, leading to spin tunnelling. A spin-transfer torque is then exerted onto the molecular spin by the inelastic spin currents and is not included in the spin dynamics, since it is compensated externally, so that the spin precession remains steady. As a back action, the anisotropic molecular spin pumps spin currents into the leads. The spin currents, noise of  $z$ -polarized spin current, spin-transfer torque, the Gilbert damping and other torque coefficients are calculated using the the Keldysh NEGF technique.<sup>80–82</sup> In the given setup, the initially single level molecular orbital results in four quasienergy levels dependent on the uniaxial magnetic anisotropy parameter,<sup>131</sup> obtained by the Floquet theorem.<sup>132–135</sup> While the elastic spin currents are driven by the bias voltage, only the inelastic spin currents driven by the molecular spin precession, involving electron spin-flips and energy change that depends on the anisotropy parameter, contribute to the spin-transfer torque. The setup can be used to generate spin currents and spin-transfer torque, and control them by adjusting the magnetic anisotropy parameter, the tilt angle of the molecular spin from the magnetic field and the Larmor frequency. Furthermore, if the anisotropy contribution to the precession frequency coincides with the Larmor frequency, the precession is suppressed, and consequently, the spin-transfer torque vanishes. Additionally, the spin-current and noise, spin-transfer torque, and torque coefficients vanish for large values of the anisotropy parameter, and can be controlled by the anisotropy parameter in the absence of the magnetic field as well.

The remainder of the article is organised as follows. The model setup of the system is introduced in Section II. The theoretical framework based on the Keldysh NEGF technique, used to calculate expressions for spin currents, noise of  $z$ -polarized spin current and spin-transfer torque is presented in Section III. The results are discussed in Section IV, where the dependence of the  $z$ -polarized spin current, corresponding autocorrelation noise, spin-transfer torque and torque coefficients, on the uniaxial magnetic anisotropy parameter, bias voltage, and Larmor frequency, are analysed at zero temperature. The conclusions are given in Section V.

## II. MODEL SETUP

The junction consists of a single orbital of an anisotropic molecule in a magnetic field, connected to two noninteracting metallic leads (see Fig. 1). The magnetic field is constant, directed along  $z$ -axis,  $\vec{B} = B\vec{e}_z$ , and does not affect the leads (left and right) with chemical potentials  $\mu_\xi$ , with  $\xi = L, R$ . The system Hamiltonian is given by  $\hat{H} = \hat{H}_L + \hat{H}_R + \hat{H}_T + \hat{H}_{MO} + \hat{H}_S$ . The first two terms represent Hamiltonians of the leads,

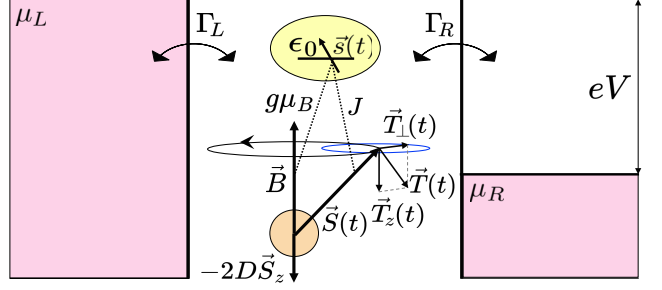


FIG. 1: (Color online) Spin tunnelling through a single molecular orbital with energy  $\epsilon_0$ , coupled to the molecular spin  $\vec{S}(t)$  with anisotropy parameter  $D$ , via exchange interaction with the coupling constant  $J$ , in the presence of a magnetic field  $\vec{B}$ , connected to two leads with chemical potentials  $\mu_L$  and  $\mu_R$ ,  $eV = \mu_L - \mu_R$ , with tunnel rates  $\Gamma_L$  and  $\Gamma_R$ . The molecular spin  $\vec{S}(t)$  precesses around the magnetic field axis with frequency  $\omega = \omega_L - 2DS_z$ . The spin-transfer torque  $\vec{T}(t)$  is exerted on the spin  $\vec{S}(t)$  by the spin currents from the leads.

$\hat{H}_\xi = \sum_{k,\sigma} \epsilon_{k\xi} \hat{c}_{k\sigma\xi}^\dagger \hat{c}_{k\sigma\xi}$ , with  $\sigma = \uparrow, \downarrow = 1, 2 = \pm 1$  denoting the electron spin state (up or down). The third term in the Hamiltonian,  $\hat{H}_T$ , represents the tunnel coupling between the orbital of the molecule and the leads, and can be written as  $\hat{H}_T = \sum_{k,\sigma,\xi} [V_{k\xi} \hat{c}_{k\sigma\xi}^\dagger \hat{d}_\sigma + V_{k\xi}^* \hat{d}_\sigma^\dagger \hat{c}_{k\sigma\xi}]$ , with matrix element  $V_{k\xi}$ , and creation (annihilation) operators of the electrons in the leads and orbital  $\hat{c}_{k\sigma\xi}^\dagger$  ( $\hat{c}_{k\sigma\xi}$ ) and  $\hat{d}_\sigma^\dagger$  ( $\hat{d}_\sigma$ ). The Hamiltonian of the molecular orbital  $\hat{H}_{MO}$  consists of three terms, one representing the noninteracting orbital with energy  $\epsilon_0$ , the second one representing the spin of the electron in the orbital in the presence of the magnetic field, and the third term representing the exchange interaction between spins of the electron in the orbital and the molecular magnet, with the exchange coupling constant  $J$ ,  $\hat{H}_{MO} = \sum_\sigma \epsilon_0 \hat{d}_\sigma^\dagger \hat{d}_\sigma + (g\mu_B/\hbar) \hat{s}\vec{B} + J\hat{s}\vec{S}$ . The spin of the electron in the molecular orbital is given by  $\hat{s} = (\hbar/2) \sum_{\sigma\sigma'} (\hat{\sigma})_{\sigma\sigma'} \hat{d}_\sigma^\dagger \hat{d}_{\sigma'}$ , with the vector of the Pauli matrices  $\hat{\sigma} = (\hat{\sigma}_x, \hat{\sigma}_y, \hat{\sigma}_z)^T$ . The constants  $g$  and  $\mu_B$  are the gyromagnetic ratio of the electron, which is assumed to be equal to the one of the molecular spin, and the Bohr magneton. The last term in the model Hamiltonian describes the Hamiltonian of the anisotropic spin of the molecule,  $\hat{H}_S = (g\mu_B/\hbar) \hat{S}\vec{B} - D\hat{S}_z^2$ , with molecular spin operator  $\hat{S} = \hat{S}_x\vec{e}_x + \hat{S}_y\vec{e}_y + \hat{S}_z\vec{e}_z$ . Here, the uniaxial magnetic anisotropy parameter is given by  $D$  and  $\vec{e}_j$  is the unit vector along the axis  $j$ , with  $j = x, y, z$ .

The spin of the magnetic molecule is large and regarded as a classical variable  $\vec{S}$ , with constant length  $S = |\vec{S}| \gg \hbar$ , neglecting the quantum fluctuations. The vector  $\vec{S}$  is the expectation value of the previously mentioned molecular spin operator,  $\vec{S} = \langle \hat{S} \rangle$ , with the dynamics expressed by the Heisenberg equation of motion  $\dot{\vec{S}} = \langle \dot{\hat{S}} \rangle = (i/\hbar) \langle [\hat{H}, \hat{S}] \rangle$ . In order to keep the molecu-

lar spin dynamics unaffected by the loss of the magnetic energy due to the exchange interaction with the spin of the tunnelling electrons, one needs to use external means, e.g., radiofrequency fields.<sup>136</sup> Taking into account the Larmor precession frequency around the magnetic field axis  $\vec{B}$ ,  $\omega_L = (g\mu_B/\hbar)B$ , the obtained equation  $\dot{\vec{S}} = (g\mu_B/\hbar)\vec{B} \times \vec{S} - 2D\vec{S}_z \times \vec{S}$  shows that the molecular spin precesses around  $z$ -axis with frequency  $\omega = \omega_L - 2DS_z$ . Compared to the isotropic molecular spin with the Larmor precession, the frequency at which the anisotropic spin precesses is modified by a term  $-2DS_z$  representing the effect of the uniaxial magnetic anisotropy on its motion. The dynamics of the molecular spin can be expressed as  $\vec{S}(t) = S_\perp \cos(\omega t)\vec{e}_x + S_\perp \sin(\omega t)\vec{e}_y + S_z\vec{e}_z$ , with  $S_\perp = S \sin\theta$  and  $S_z = S \cos\theta$ , where  $\theta$  is the tilt angle between the positive direction along  $z$ -axis and  $\vec{S}$ . While the precession of the molecular spin is kept undamped, i.e., the spin-transfer torque exerted on it by the flow of electron spins from the leads is externally compensated, the precessing molecular spin affects spin of the itinerant electrons during the exchange interaction, as a back action, thus pumping spin currents into the leads and having an impact on spin-transport properties of the junction.

### III. THEORETICAL FRAMEWORK

#### A. Spin Current

The spin-current operators of the lead  $\xi$  are given by the Heisenberg equation

$$\hat{I}_{\xi j}(t) = \frac{\hbar}{2} \frac{d\hat{N}_{\xi j}}{dt} = \frac{i}{2} [\hat{H}, \hat{N}_{\xi j}], \quad (1)$$

where  $j = x, y, z$  denote the component of the spin current with electronic spins oriented along the given spatial direction,  $[\cdot, \cdot]$  symbolizes the commutator, whereas  $\hat{N}_{\xi j} = \sum_{k,\sigma,\sigma'} \hat{c}_{k\sigma\xi}^\dagger (\hat{\sigma}_j)_{\sigma\sigma'} \hat{c}_{k\sigma\xi}$  denotes the spin occupation number operator of the lead  $\xi$ , with matrix elements of the Pauli operators  $(\hat{\sigma}_j)_{\sigma\sigma'}$ . The average spin current from the contact  $\xi$ , as a flow of electron spins oriented along  $j$  spatial direction to the orbital of the magnetic molecule can be written as

$$I_{\xi j}(t) = \frac{1}{2} \left\langle \frac{d}{dt} \hat{N}_{\xi j} \right\rangle = \frac{i}{2} \langle [\hat{H}, \hat{N}_{\xi j}] \rangle, \quad (2)$$

in units in which  $\hbar = e = 1$ . Employing the Keldysh nonequilibrium Green's functions technique,<sup>81,82</sup> the components of the spin current can be calculated as

$$I_{\xi j}(t) = -\text{Re} \int dt' \text{Tr} \left\{ \hat{\sigma}_j [\hat{G}^r(t, t') \hat{\Sigma}_\xi^<(t', t) + \hat{G}^<(t, t') \hat{\Sigma}_\xi^a(t', t)] \right\}. \quad (3)$$

Here,  $\hat{G}^{r,a,<,>}(t, t')$  denote the retarded, advanced, lesser, and greater Green's functions of the spin carriers in the molecular orbital. The matrix elements

of the Green's functions are given by  $G_{\sigma\sigma'}^{r,a}(t, t') = \mp i\theta(\pm t \mp t') \langle \{ \hat{d}_\sigma(t), \hat{d}_{\sigma'}^\dagger(t') \} \rangle$ ,  $G_{\sigma\sigma'}^<(t, t') = i \langle \hat{d}_{\sigma'}^\dagger(t') \hat{d}_\sigma(t) \rangle$  and  $G_{\sigma\sigma'}^>(t, t') = -i \langle \hat{d}_\sigma(t) \hat{d}_{\sigma'}^\dagger(t') \rangle$ , where  $\{ \cdot, \cdot \}$  symbolizes the anticommutator. The self-energies from the tunnel coupling between the orbital and lead  $\xi$  are represented by  $\hat{\Sigma}_\xi^{r,a,<,>}(t, t')$ , with diagonal matrix elements in the electron spin space with respect to the basis of the eigenstates of  $\hat{s}_z$ . Their nonzero matrix elements can be expressed as  $\Sigma_\xi^{r,a,<,>}(t, t') = \sum_k V_{k\xi} g_{k\xi}^{r,a,<,>}(t, t') V_{k\xi}^*$ , with  $g_{k\xi}^{r,a,<,>}(t, t')$  denoting the Green's functions of the spin carriers (electrons) in the lead  $\xi$ . Applying the double Fourier transformations in Eq. (3), it can be further simplified as

$$I_{\xi j}(t) = \Gamma_\xi \text{Im} \int \frac{d\epsilon}{2\pi} \int \frac{d\epsilon'}{2\pi} e^{-i(\epsilon - \epsilon')t} \times \text{Tr} \left\{ \hat{\sigma}_j \left[ f_\xi(\epsilon') \hat{G}^r(\epsilon, \epsilon') + \frac{1}{2} \hat{G}^<(\epsilon, \epsilon') \right] \right\}, \quad (4)$$

with the tunnel coupling between the orbital and lead  $\xi$ ,  $\Gamma_\xi(\epsilon) = 2\pi \sum_k |V_{k\xi}|^2 \delta(\epsilon - \epsilon_{k\xi})$ , which is energy independent and constant in the wide-band limit. The Fermi-Dirac distribution of the spin carriers in the lead  $\xi$  is given by  $f_\xi(\epsilon) = [e^{(\epsilon - \mu_\xi)/k_B T} + 1]^{-1}$ , where  $T$  and  $k_B$  are the temperature and the Boltzmann constant.

The retarded Green's function of the spin carriers in the orbital of the molecule can be calculated applying Dyson's expansion and analytic continuation rules.<sup>82</sup> Its double-Fourier transformed matrix elements can be expressed as<sup>89,131,137</sup>

$$G_{\sigma\sigma}^r(\epsilon, \epsilon') = \frac{2\pi\delta(\epsilon - \epsilon') G_{\sigma\sigma}^{0r}(\epsilon)}{1 - \gamma^2 G_{\sigma\sigma}^{0r}(\epsilon) G_{-\sigma-\sigma}^{0r}(\epsilon_\sigma)}, \quad (5)$$

$$G_{\sigma-\sigma}^r(\epsilon, \epsilon') = \frac{2\pi\gamma\delta(\epsilon_\sigma - \epsilon') G_{\sigma\sigma}^{0r}(\epsilon) G_{-\sigma-\sigma}^{0r}(\epsilon_\sigma)}{1 - \gamma^2 G_{\sigma\sigma}^{0r}(\epsilon) G_{-\sigma-\sigma}^{0r}(\epsilon_\sigma)}, \quad (6)$$

with  $\epsilon_\sigma = \epsilon - \sigma\omega = \epsilon - \sigma(\omega_L - 2DS_z)$ ,  $\gamma = JS \sin(\theta)/2$ . The retarded Green's function of the spin carriers in the molecular orbital in the presence of the static molecular spin  $S = S_z$ , calculated using the equation of motion technique,<sup>138</sup> and the Fourier transformations, is given by  $\hat{G}^{0r}(\epsilon) = [\epsilon - \epsilon_0 - \Sigma^r - \hat{\sigma}_z(g\mu_B B + JS_z)/2]^{-1}$ ,<sup>121,137</sup> where  $\Sigma^{r,a} = \mp i\Gamma/2$  and  $\Gamma = \sum_\xi \Gamma_\xi$ . The Green's functions  $\hat{G}^{<,>}(\epsilon, \epsilon')$  can be obtained using the double-Fourier transformed Keldysh equation, expressed as  $\hat{G}^{<,>}(\epsilon, \epsilon') = \int d\epsilon'' \hat{G}^r(\epsilon, \epsilon'') \hat{\Sigma}^{<,>}(\epsilon'', \epsilon') \hat{G}^a(\epsilon'', \epsilon')/2\pi$ ,<sup>82</sup> with lesser self-energy  $\Sigma^<(\epsilon) = i \sum_\xi \Gamma_\xi f_\xi(\epsilon)$ , greater self-energy  $\Sigma^>(\epsilon) = i \sum_\xi \Gamma_\xi (f_\xi(\epsilon) - 1)$  and advanced Green's function  $\hat{G}^a(\epsilon, \epsilon') = [\hat{G}^r(\epsilon', \epsilon)]^\dagger$ .

At last, the spin current given by Eq. (4) can be calculated using the above expressions for the Green's functions  $\hat{G}^r(\epsilon, \epsilon')$  and  $\hat{G}^<(\epsilon, \epsilon')$  and has time-dependent  $I_{\xi x}(t)$  and  $I_{\xi y}(t)$  components, obtained as

$$I_{\xi x}(t) = I_{\xi x}(D) e^{-i(\omega_L - 2DS_z)t} + I_{\xi x}^*(D) e^{i(\omega_L - 2DS_z)t}, \quad (7)$$

$$I_{\xi y}(t) = I_{\xi y}(D) e^{-i(\omega_L - 2DS_z)t} + I_{\xi y}^*(D) e^{i(\omega_L - 2DS_z)t}, \quad (8)$$

while  $I_{\xi z}$  is time-independent. The expressions for the the spin current component  $I_{\xi z}$  and the complex functions  $I_{\xi x}(D)$  and  $I_{\xi y}(D)$ , are presented by Eqs. (A1)–(A3) in the Appendix. For the isotropic molecular spin ( $D = 0$ ), they reduce to the expressions obtained before.<sup>89</sup>

In the presence of the precessing anisotropic molecular spin  $\vec{S}(t)$  and the external magnetic field  $\vec{B}$ , the initial single resonant transmission channel with energy  $\epsilon_0$ , results in four channels available for spin transport, located at Floquet quasienergies<sup>131</sup>

$$\epsilon_{1,3} = \epsilon_0 - \frac{\omega_L}{2} + DS_z \pm \sqrt{D(D+J)S_z^2 + \left(\frac{JS}{2}\right)^2}, \quad (9)$$

$$\epsilon_{2,4} = \epsilon_0 + \frac{\omega_L}{2} - DS_z \pm \sqrt{D(D+J)S_z^2 + \left(\frac{JS}{2}\right)^2}, \quad (10)$$

obtained using the Floquet theorem,<sup>132–135</sup> since the Hamiltonian of the molecular orbital is a periodic function of time  $\hat{H}_{MO}(t) = \hat{H}_{MO}(t + 2\pi/\omega)$ . Periodic motion of the molecular spin leads to the absorption (emission) of an energy quantum  $\omega$  by the spin-carrying electron in the orbital, which is accompanied by a spin-flip, i.e., as a result of the exchange interaction between the spin of the molecule and spin of the itinerant electron, the state with quasienergy  $\epsilon_1(\epsilon_3)$  is coupled to the state with quasienergy  $\epsilon_2(\epsilon_4) = \epsilon_1(\epsilon_3) + \omega = \epsilon_1(\epsilon_3) + \omega_L - 2DS_z$  and opposite spin.

## B. Noise of z-polarized Spin Current

In order to obtain further characteristics of spin transport, one can study spin-current noise. As a complement to Ref. [131], where the charge-current noise was discussed, the noise of spin current polarized along the  $z$ -direction is calculated here. Since only the tun-

ing Hamiltonian  $\hat{H}_T$  contributes to the commutator in Eq. (1), the resulting spin-current operator  $\hat{I}_{\xi z}(t)$  is given by

$$\hat{I}_{\xi z}(t) = \frac{i}{2} \sum_{\sigma} (-1)^{\sigma} \hat{I}_{\xi \sigma}(t), \quad (11)$$

where the operator component  $\hat{I}_{\xi \sigma}(t)$  reads

$$\hat{I}_{\xi \sigma}(t) = \sum_k [V_{k\xi} \hat{c}_{k\sigma\xi}^{\dagger}(t) \hat{d}_{\sigma}(t) - V_{k\xi}^* \hat{d}_{\sigma}^{\dagger}(t) \hat{c}_{k\sigma\xi}(t)]. \quad (12)$$

The spin-current fluctuation operator  $\delta\hat{I}_{\xi z}(t)$  in lead  $\xi$ , can be written as

$$\delta\hat{I}_{\xi z}(t) = \hat{I}_{\xi z}(t) - \langle \hat{I}_{\xi z}(t) \rangle. \quad (13)$$

The nonsymmetrized noise of  $z$ -polarized spin current, defined as correlation between fluctuations of  $z$ -polarized spin currents in contacts  $\xi$  and  $\zeta$ , is given by<sup>82,139</sup>

$$S_{\xi\zeta}^{zz}(t, t') = \langle \delta\hat{I}_{\xi z}(t) \delta\hat{I}_{\zeta z}(t') \rangle. \quad (14)$$

According to Eqs. (11) and (13), the noise of  $z$ -polarized spin current equals

$$S_{\xi\zeta}^{zz}(t, t') = \frac{1}{4} \sum_{\sigma\sigma'} (-1)^{\delta_{\sigma\sigma'}} S_{\xi\zeta}^{\sigma\sigma'}(t, t'), \quad (15)$$

with  $S_{\xi\zeta}^{\sigma\sigma'}(t, t') = \langle \delta\hat{I}_{\xi \sigma}(t) \delta\hat{I}_{\zeta \sigma'}(t') \rangle$ . Implementing the Wick's theorem<sup>140</sup> and Langreth analytical continuation rules<sup>141</sup> to the correlation function  $S_{\xi\zeta}^{\sigma\sigma'}(t, t')$  in Eq. (15), and using the Green's functions of the molecular orbital and the self-energies from the tunnel couplings between the orbital and the leads, one obtains the expression for the noise of spin current.<sup>95</sup> Employing the Fourier transforms of the Green's functions,  $G_{\sigma\sigma'}^{r,a,<,>}(\epsilon, \epsilon')$ , and self-energies  $\Sigma_{\xi}^{r,a,<,>}(\epsilon)$ , the expression for the noise of  $z$ -polarized spin current<sup>95</sup> can be transformed into

$$\begin{aligned} S_{\xi\zeta}^{zz}(t, t') = & \frac{1}{4} \sum_{\sigma\sigma'} (-1)^{\delta_{\sigma\sigma'}} \left\{ \int \frac{d\epsilon_1}{2\pi} \int \frac{d\epsilon_2}{2\pi} \int \frac{d\epsilon_3}{2\pi} \int \frac{d\epsilon_4}{2\pi} e^{-i(\epsilon_1 - \epsilon_2)t} e^{i(\epsilon_3 - \epsilon_4)t'} \right. \\ & \times \left\{ [G_{\sigma\sigma'}^r(\epsilon_1, \epsilon_3) \Sigma_{\zeta}^>(\epsilon_3) + 2G_{\sigma\sigma'}^>(\epsilon_1, \epsilon_3) \Sigma_{\zeta}^a] [G_{\sigma'\sigma}^r(\epsilon_4, \epsilon_2) \Sigma_{\xi}^<(\epsilon_2) + 2G_{\sigma'\sigma}^<(\epsilon_4, \epsilon_2) \Sigma_{\xi}^a] \right. \\ & + [\Sigma_{\xi}^>(\epsilon_1) G_{\sigma\sigma'}^a(\epsilon_1, \epsilon_3) + 2G_{\sigma\sigma'}^>(\epsilon_1, \epsilon_3) \Sigma_{\xi}^r] [\Sigma_{\zeta}^<(\epsilon_4) G_{\sigma'\sigma}^a(\epsilon_4, \epsilon_2) + 2G_{\sigma'\sigma}^<(\epsilon_4, \epsilon_2) \Sigma_{\zeta}^r] \\ & \left. + 4\Sigma_{\xi}^r \Sigma_{\zeta}^a G_{\sigma\sigma'}^>(\epsilon_1, \epsilon_3) G_{\sigma'\sigma}^<(\epsilon_4, \epsilon_2) \right\} \\ & - \delta_{\xi\zeta} \delta_{\sigma\sigma'} \int \frac{d\epsilon_1}{2\pi} \int \frac{d\epsilon_2}{2\pi} \int \frac{d\epsilon_3}{2\pi} \\ & \times \left\{ e^{-i(\epsilon_1 - \epsilon_3)t} e^{i(\epsilon_2 - \epsilon_3)t'} G_{\sigma\sigma'}^>(\epsilon_1, \epsilon_2) \Sigma_{\xi}^<(\epsilon_3) \right. \\ & \left. + e^{-i(\epsilon_1 - \epsilon_3)t} e^{i(\epsilon_1 - \epsilon_2)t'} \Sigma_{\xi}^>(\epsilon_1) G_{\sigma'\sigma}^<(\epsilon_2, \epsilon_3) \right\} \left. \right\}, \quad (16) \end{aligned}$$

and, as it depends only on the time difference  $\tau = t - t'$ , its power spectrum equals

$$S_{\xi\zeta}^{zz}(\Omega) = \int d\tau e^{i\Omega\tau} S_{\xi\zeta}^{zz}(\tau). \quad (17)$$

Since it is of experimental interest, the zero-frequency

noise power of  $z$ -polarized spin-current  $S_{LL}^{zz} = S_{LL}^{zz}(0)$  will be analyzed at zero temperature in Section IV.

### C. Spin-transfer torque

In the presence of the anisotropic molecular spin  $\vec{S}(t)$ , interacting with the incoming flow of electron spins from the leads via exchange interactions, the transfer of spin angular momentum to the molecular spin occurs, resulting in the spin-transfer torque  $\vec{T}(t)$  exerted on the molecular spin. As already mentioned, the spin transfer torque

is compensated by external means, so that the molecular spin precession remains unaffected. But, since the total spin angular momentum is conserved, as a back action, the spin of the molecule generates a torque  $-\vec{T}(t)$  on the spin currents from the leads,<sup>36,49,50,67</sup>

$$-\vec{T}(t) = \vec{I}_L(t) + \vec{I}_R(t), \quad (18)$$

where  $\vec{I}_\xi(t) = \sum_j I_{\xi j}(t) \vec{e}_j$ , while  $\vec{T}(t) = \sum_j T_j \vec{e}_j$ . Employing Eqs. (7), (8), (18) and Eqs. (A1)–(A3) given in the Appendix, the spin-transfer torque spatial components  $T_j$  can be expressed as

$$T_x(t) = - \int \frac{d\epsilon}{2\pi} \sum_{\xi\zeta} \frac{\Gamma_\xi \Gamma_\zeta}{\Gamma} [f_\xi(\epsilon - \omega_L + 2DS_z) - f_\zeta(\epsilon)] \times \text{Im} \left\{ \frac{\gamma G_{11}^{0r}(\epsilon) G_{22}^{0a}(\epsilon - \omega_L + 2DS_z)}{|1 - \gamma^2 G_{11}^{0r}(\epsilon) G_{22}^{0r}(\epsilon - \omega_L + 2DS_z)|^2} \right. \\ \left. \times [1 - \gamma^2 G_{11}^{0a}(\epsilon) G_{22}^{0r}(\epsilon - \omega_L + 2DS_z)] e^{-i(\omega_L - 2DS_z)t} \right\}, \quad (19)$$

$$T_y(t) = - \int \frac{d\epsilon}{2\pi} \sum_{\xi\zeta} \frac{\Gamma_\xi \Gamma_\zeta}{\Gamma} [f_\xi(\epsilon - \omega_L + 2DS_z) - f_\zeta(\epsilon)] \times \text{Re} \left\{ \frac{\gamma G_{11}^{0r}(\epsilon) G_{22}^{0a}(\epsilon - \omega_L + 2DS_z)}{|1 - \gamma^2 G_{11}^{0r}(\epsilon) G_{22}^{0r}(\epsilon - \omega_L + 2DS_z)|^2} \right. \\ \left. \times [1 - \gamma^2 G_{11}^{0a}(\epsilon) G_{22}^{0r}(\epsilon - \omega_L + 2DS_z)] e^{-i(\omega_L - 2DS_z)t} \right\}, \quad (20)$$

$$T_z = - \int \frac{d\epsilon}{2\pi} \sum_{\xi\zeta} \Gamma_\xi \Gamma_\zeta [f_\xi(\epsilon - \omega_L + 2DS_z) - f_\zeta(\epsilon)] \times \frac{\gamma^2 |G_{11}^{0r}(\epsilon) G_{22}^{0r}(\epsilon - \omega_L + 2DS_z)|^2}{|1 - \gamma^2 G_{11}^{0r}(\epsilon) G_{22}^{0r}(\epsilon - \omega_L + 2DS_z)|^2}. \quad (21)$$

In the limit  $|D| \ll |\omega_L/2S_z|$ , Eqs. (19)–(21) reduce to the previously calculated expressions for the spatial components of the spin-transfer torque.<sup>89</sup> Also, if the magnetic field is turned off, with  $\omega_L = 0$ , in the junction with the isotropic molecular spin ( $D = 0$ ), the exerted spin-transfer torque vanishes,  $\vec{T}(t) = 0$ ,<sup>89</sup> while, according to Eqs. (19)–(21),  $\vec{T}(t) \neq 0$  if the molecular spin is anisotropic ( $D \neq 0$ ). Both  $T_x(t)$  and  $T_y(t)$  can be written as  $T_x(t) = T_x \cos(\omega t + \phi_x)$  and  $T_y(t) = T_y \cos(\omega t + \phi_y)$ , with the phase difference  $\phi_x - \phi_y = \pi/2$ , and  $T_x, T_y$  the amplitudes of the given spin-transfer torque components. Since the amplitudes are equal, it is convenient to introduce the in-plane torque component, which is orthogonal to the  $z$ -axis,  $\vec{T}_\perp(t) = \vec{T}_x(t) + \vec{T}_y(t)$ , while

$$\vec{T}(t) = \vec{T}_\perp(t) + \vec{T}_z(t). \quad (22)$$

The in-plane component of the spin transfer torque,  $\vec{T}_\perp(t)$ , precesses around the end point of the molecular

spin  $\vec{S}(t)$  in the  $xy$  plane (see Fig. 1), and has a constant magnitude  $|\vec{T}_\perp(t)| = T_\perp = T_x = T_y$ .

In relation to the molecular spin  $\vec{S}(t)$ , the spin-transfer torque reads

$$\vec{T}(t) = \frac{\alpha}{S} \dot{\vec{S}}(t) \times \vec{S}(t) + \beta \dot{\vec{S}}(t) + \eta \vec{S}(t), \quad (23)$$

where the Gilbert damping component of the torque, given by the first term, tends to align the anisotropic molecular spin  $\vec{S}(t)$  anti(parallel) to the direction of the effective magnetic field  $\vec{B}_{\text{eff}} = \vec{B} - (2D/g\mu_B) \vec{S}_z$  and dissipate(add) magnetic energy, with  $\alpha$ , the Gilbert damping coefficient, while the second term with coefficient  $\beta$  represents the change of the precession frequency of the molecular spin  $\vec{S}(t)$ , and the contribution in the third term is characterized by the coefficient  $\eta$ . Combining expressions given by Eqs. (19)–(23), the resulting spin-transfer-torque coefficients  $\alpha$  and  $\beta$  can be written as

$$\alpha = -\frac{1}{(\omega_L - 2DS_z)S} \int \frac{d\epsilon}{2\pi} \sum_{\xi\zeta} \Gamma_\xi \Gamma_\zeta [f_\xi(\epsilon - \omega_L + 2DS_z) - f_\zeta(\epsilon)]$$

$$\times \frac{(JS_z/2\Gamma)\text{Im}\{G_{11}^{0r}(\epsilon)G_{22}^{0a}(\epsilon - \omega_L + 2DS_z)\} - \gamma^2|G_{11}^{0r}(\epsilon)G_{22}^{0r}(\epsilon - \omega_L + 2DS_z)|^2}{|1 - \gamma^2 G_{11}^{0r}(\epsilon)G_{22}^{0r}(\epsilon - \omega_L + 2DS_z)|^2}, \quad (24)$$

$$\beta = -\frac{J}{\omega_L - 2DS_z} \int \frac{d\epsilon}{4\pi} \sum_{\xi\zeta} \frac{\Gamma_\xi \Gamma_\zeta}{\Gamma} [f_\xi(\epsilon - \omega_L + 2DS_z) - f_\zeta(\epsilon)]$$

$$\times \frac{\text{Re}\{G_{11}^{0r}(\epsilon)G_{22}^{0a}(\epsilon - \omega_L + 2DS_z)\} - \gamma^2|G_{11}^{0r}(\epsilon)G_{22}^{0r}(\epsilon - \omega_L + 2DS_z)|^2}{|1 - \gamma^2 G_{11}^{0r}(\epsilon)G_{22}^{0r}(\epsilon - \omega_L + 2DS_z)|^2}, \quad (25)$$

while the coefficient in the third term of Eq.(23),  $\eta$ , can be expressed in terms of  $T_z$  and Gilbert damping coefficient  $\alpha$  as

$$\eta = \frac{T_z}{S_z} + \frac{4\gamma^2(\omega_L - 2DS_z)}{J^2 S S_z} \alpha. \quad (26)$$

In the limit  $|D| \ll |\omega_L/2S_z|$ , the effect of the uniaxial magnetic anisotropy on the spin-transfer torque can be neglected and Eqs. (24)–(26) are in agreement with the Gilbert damping coefficient  $\alpha$  and coefficients  $\beta$  and  $\eta$  obtained for the isotropic molecular spin.<sup>89</sup> Finally, the magnitude of the in-plane spin-transfer torque component  $T_\perp$  can be expressed using  $\alpha$ ,  $\beta$  and  $T_z$  as follows

$$T_\perp = \frac{2|\gamma(\omega_L - 2DS_z)|}{J} \sqrt{\beta^2 + \frac{1}{S_z^2} \left[ S\alpha + \frac{T_z}{(\omega_L - 2DS_z)} \right]^2} \quad (27)$$

For a static spin,  $\omega = 0$ , that is  $D = \omega_L/2S_z$ , the spin-transfer torque  $\vec{T}(t) = \vec{0}$ . The characteristics of spin-transfer torque exerted on the anisotropic molecular spin in the given setup, and the corresponding torque coefficients at zero temperature, will be analysed in the next section.

#### IV. RESULTS AND DISCUSSION

In this section, the properties of the  $z$ -polarized spin current  $I_{Lz}$  and autocorrelation zero-frequency noise  $S_{LL}^{zz}$  at zero temperature are discussed. Then, the characteristics of the spin-transfer torque generated on the anisotropic molecular spin by the spin currents from the leads and torque coefficients are analyzed as functions of the uniaxial magnetic anisotropy parameter  $D$ , bias voltage  $eV = \mu_L - \mu_R$  and Larmor frequency  $\omega_L$ , for different values of the parameter  $D$ , at zero temperature.

In Fig. 2, the spin current  $I_{Lz}$  and auto-correlation zero-frequency noise power of the spin current polarized along the  $z$ -direction,  $S_{LL}^{zz}$ , are plotted as functions of the uniaxial magnetic anisotropy parameter  $D$ , for different tilt angles  $\theta$ , at zero bias conditions, with chemical potentials of the leads  $\mu = \mu_L = \mu_R = 0.1\epsilon_0$ , and zero temperature. For a static molecular spin with  $\theta = 0$

(purple dotted lines in Fig. 2), according to Eq. (A3) in the Appendix, the spin current  $I_{Lz}$  is equal to zero, as well as noise  $S_{LL}^{zz}$ , since  $\gamma = 0$ . In the case of  $\theta = \pi/2$  (pink dashed lines in Fig. 2), the spin current  $I_{Lz}$  and noise  $S_{LL}^{zz}$  are independent of  $D$ , since  $S_z = 0$ . For  $\theta = \pi/3$  and  $\omega_L = 0.5\epsilon_0$  (green lines in Fig. 2) one notices maximums in  $I_{Lz}$  and  $S_{LL}^{zz}$  around  $D = -0.00431\epsilon_0$ , corresponding to  $\mu_L = \mu_R = \epsilon_3$ , and a minimum in  $I_{Lz}$  and local maximum in  $S_{LL}^{zz}$  around  $D = 0.00766\epsilon_0$ , corresponding to  $\mu_L = \mu_R = \epsilon_4$  (grid lines), while for  $-0.00431 < D < 0.00766$ , all four quasienergy levels  $\epsilon_i$ ,  $i \in \{1, 2, 3, 4\}$ , lie above the chemical potentials  $\mu$ , so that both spin current  $I_{Lz}$  and shot noise  $S_{LL}^{zz}$  drop to zero, taking into account the level broadening  $\Gamma$ . The spin current  $I_{Lz}$  and noise  $S_{LL}^{zz}$  vanish at  $D = \omega_L/2S_z$ , e.g., at  $D = 0.005\epsilon_0$  for  $\theta = \pi/3$  (middle grid line intersects with green line in Fig. 2), i.e., for  $\omega = 0$ , as without molecular spin precession at zero-bias conditions, elastic and inelastic tunnelling processes do not occur. The spin current  $I_{Lz} > 0$  for  $D < \omega_L/2S_z$  ( $\omega > 0$ ) since levels  $\epsilon_3$  (spin-down) and  $\epsilon_4$  (spin-up) satisfy  $\epsilon_3 < \epsilon_4$ , leading to positive spin-up component of spin current  $I_{Lz}^\uparrow = -I_{Lz}^\downarrow > 0$ , and increasing  $I_{Lz}$  and  $S_{LL}^{zz}$  as chemical potential  $\mu$  approaches  $\epsilon_3$ . Similarly, for  $D > \omega_L/2S_z$  ( $\omega < 0$ ), spin-down level  $\epsilon_3$  lies above spin-up level  $\epsilon_4$ ,  $\epsilon_3 > \epsilon_4$  leading to  $I_{Lz}^\uparrow = -I_{Lz}^\downarrow < 0$ , and hence  $I_{Lz} < 0$ . In the absence of a magnetic field,  $\omega_L = 0$  (orange line in Fig. 2), the molecular spin precesses around the  $z$ -axis with frequency  $\omega = -2DS_z$ , and hence,  $I_{Lz} \geq 0$  for  $D \leq 0$ , and  $I_{Lz} < 0$  for  $D > 0$ . After reaching resonances between  $\mu$  and levels  $\epsilon_3$  and  $\epsilon_4$ , while both  $\epsilon_1 > \mu$  and  $\epsilon_2 > \mu$ , with further increase of  $|D|$ , spin current  $I_{Lz}$  and shot noise  $S_{LL}^{zz}$  decrease, as more energy is needed to flip an electron spin which is already in lower quasienergy level, and for  $|D| \gg \omega_L/2S_z$  they vanish. Besides, taking into account the tunneling rate  $\Gamma$ , for  $|D| \gg \Gamma$ , the precession frequency  $|\omega| \gg \Gamma$ , so that the probability of exchange of spin angular momentum between molecular and tunneling spin is low.

The spin current  $I_{Lz}$ , and auto-correlation shot noise of spin current  $S_{LL}^{zz}$ , are presented as functions of the chemical potential of the leads  $\mu = \mu_L = \mu_R$  at zero temperature in Figs. 3(a) and 3(b), for several values of the uni-

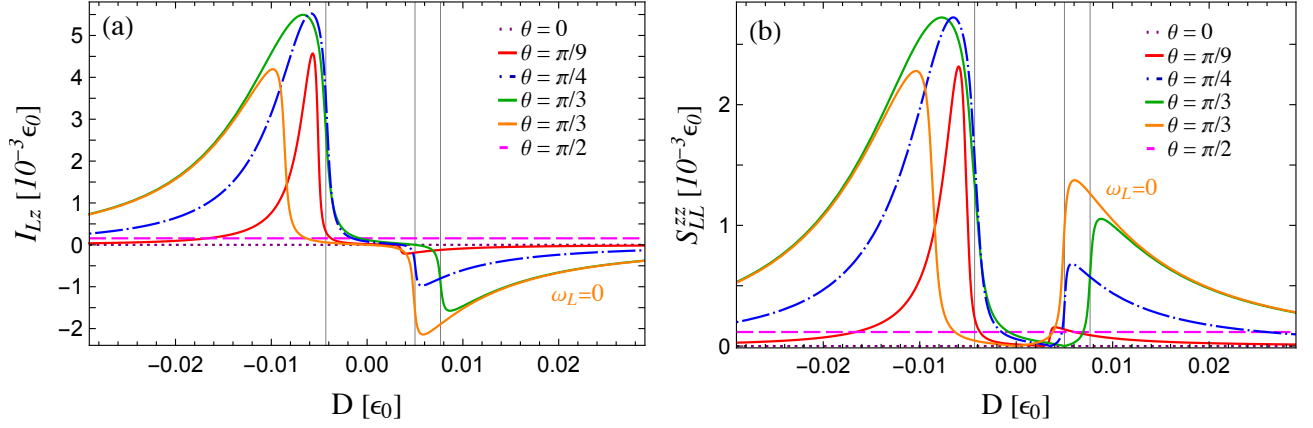


FIG. 2: (Color online) (a) Spin current  $I_{Lz}$  and (b) auto-correlation spin-current shot noise  $S_{LL}^{zz}$ , as functions of the uniaxial magnetic anisotropy parameter  $D$  for different tilt angles  $\theta$ , at zero temperature. The magnetic field  $\vec{B} = B\vec{e}_z$  and Larmor frequency  $\omega_L = 0.5 \epsilon_0$ , except for a zero magnetic field where  $\omega_L = 0$  (orange line). The chemical potentials of the leads are equal:  $\mu_L = \mu_R = 0.1 \epsilon_0$ . The other parameters are set to:  $\Gamma = 0.05 \epsilon_0$ ,  $\Gamma_L = \Gamma_R = \Gamma/2$ ,  $J = 0.01 \epsilon_0$ ,  $S = 100$ . Grid lines for  $\theta = \pi/3$  and  $\omega_L = 0.5 \epsilon_0$  (green line), are positioned at  $D = -0.00431 \epsilon_0$  ( $\mu_L = \mu_R = \epsilon_3$ ),  $D = 0.00766 \epsilon_0$  ( $\mu_L = \mu_R = \epsilon_4$ ), and  $D = 0.005 \epsilon_0$  ( $\omega = 0$ ).

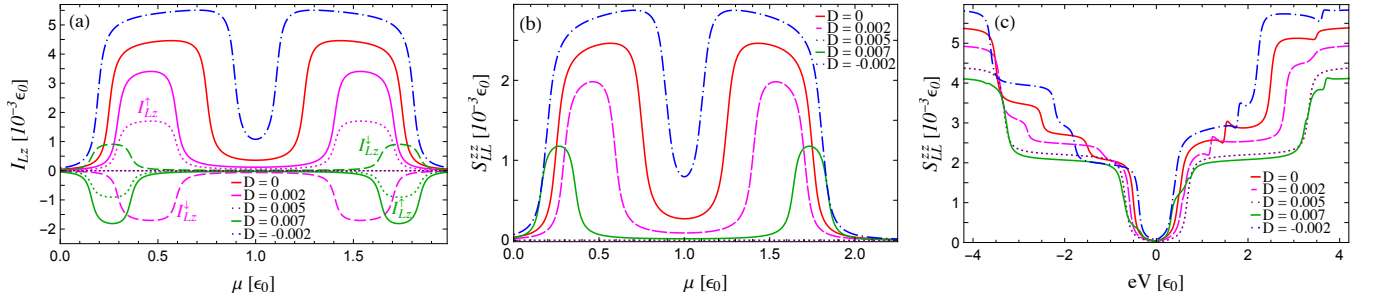


FIG. 3: (Color online) (a) Spin current  $I_{Lz}$ , (b) auto-correlation spin-current shot noise  $S_{LL}^{zz}$ , as functions of the chemical potential of the leads  $\mu = \mu_L = \mu_R$ , and (c) auto-correlation spin-current shot noise  $S_{LL}^{zz}$  as a function of the applied bias voltage  $eV = \mu_L - \mu_R$  with  $\mu_{L,R} = \pm eV/2$ , for different uniaxial magnetic anisotropy parameters  $D$ , with  $\vec{B} = B\vec{e}_z$ , at zero temperature. The other parameters are set to:  $\Gamma = 0.05 \epsilon_0$ ,  $\Gamma_L = \Gamma_R = \Gamma/2$ ,  $\omega_L = 0.5 \epsilon_0$ ,  $J = 0.01 \epsilon_0$ ,  $S = 100$ , and  $\theta = \pi/3$ . All energies are given in the units of  $\epsilon_0$ . For  $\mu_L = \mu_R$  and  $D = \omega_L/2S_z = 0.005 \epsilon_0$ ,  $I_{Lz} = 0$  and  $S_{LL}^{zz} = 0$  (purple dotted lines).

axial magnetic anisotropy parameter  $D$ . Since  $I_{Lz}^\uparrow = -I_{Lz}^\downarrow$  at zero-bias conditions, the corresponding charge current is zero, with positive charge-current noise in the regions between levels connected with spin-flips,<sup>131</sup> whereas, the shot noise of spin-current  $S_{LL}^{zz}$  is positive, while the spin current  $I_{Lz}$  takes positive values for  $D < \omega_L/2S_z$  ( $\omega > 0$ ). With the decrease of  $|\omega|$ , the magnitude of the spin current  $I_{Lz}$  and shot noise  $S_{LL}^{zz}$  decrease. In Fig. 3(c) the dependence of auto-correlation shot noise  $S_{LL}^{zz}$  on the bias voltage  $eV = \mu_L - \mu_R$ , with  $\mu_{L,R} = \pm eV/2$ , at zero temperature, is plotted for different values of the anisotropy parameter  $D$ . The steps and dip-peak features in the spin-current shot noise  $S_{LL}^{zz}$  are positioned at values of bias voltage  $eV$  such that  $\pm eV/2 = \mu_\xi = \epsilon_i$ , denoting Floquet quasienergy levels  $\epsilon_i$ , available for spin transport and, thus, depending on the magnetic anisotropy parameter  $D$ . Alike the Fano effect,<sup>142</sup> the dip-peak features in the spin-current noise  $S_{LL}^{zz}$  are present due to quantum

interference<sup>143</sup> between the states connected with inelastic spin tunnelling involving spin-flips.<sup>95</sup> For large values of  $|eV|$  spin-current noise  $S_{LL}^{zz}$  is saturated.

In Fig. 4 the Gilbert damping coefficient  $\alpha$ , the coefficient  $\beta$ , the magnitude of the in-plane component of the spin-transfer torque  $T_\perp$  and the torque along  $z$  direction,  $T_z$ , are shown as functions of the uniaxial magnetic anisotropy parameter  $D$ , for five different tilt angles  $\theta$  at zero temperature. Starting with  $\theta = 0$ , when  $S = S_z$  (purple dotted lines in Fig. 4), one notices that  $\alpha$  has two local maximums and two local minimums around values of  $D$  that correspond to resonances  $\mu_\xi = \epsilon_i$ . The coefficient  $\beta$  has four minimums at the same values of  $D$ . Taking into account that the spin of the molecule is static for  $\theta = 0$ ,  $\dot{\vec{S}}(t) = 0$ , and  $\gamma = 0$ , the spin-transfer torque component  $T_z = 0$  according to Eq. (21), and  $T_\perp = 0$  according to Eq. (27). Note the presence of the elastic spin currents here,  $I_{Lz} = -I_{Rz}$  [see Eq. (A3) in the Ap-

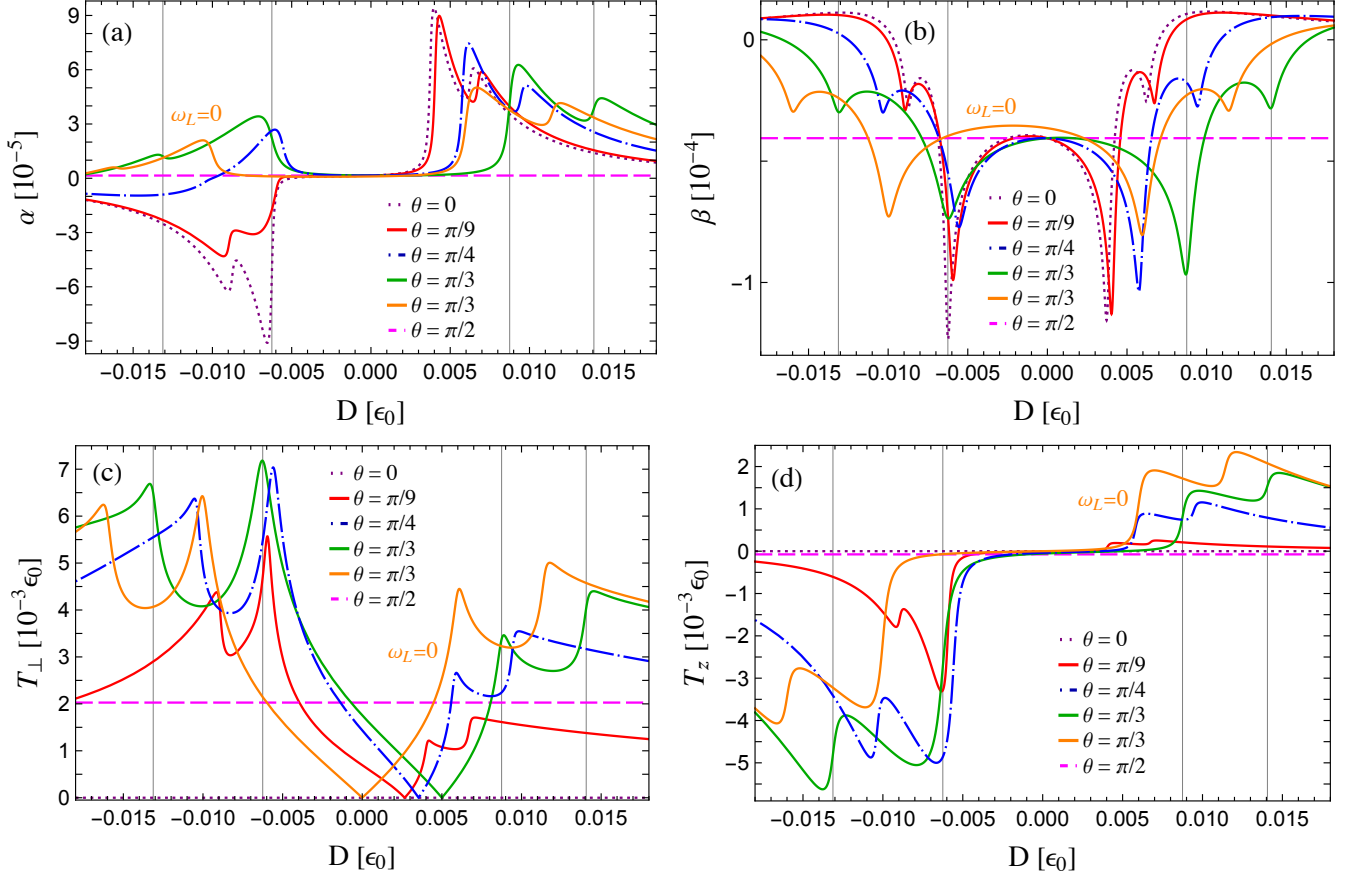


FIG. 4: (Color online) (a) Gilbert damping coefficient  $\alpha$ , (b) coefficient  $\beta$ , (c) magnitude of the in-plane component of the spin-transfer torque,  $T_{\perp}$  and (d) spatial component of the torque along  $z$ -direction  $T_z$ , as functions of the uniaxial magnetic anisotropy parameter  $D$  for different tilt angles  $\theta$ , at zero temperature. The magnetic field  $\vec{B} = B\vec{e}_z$  and Larmor frequency  $\omega_L = 0.5\epsilon_0$ , except for a zero magnetic field where  $\omega_L = 0$  (orange line). The chemical potentials of the leads are equal to:  $\mu_L = 2.5\epsilon_0$  and  $\mu_R = 0$ . The other parameters are set to:  $\Gamma = 0.05\epsilon_0$ ,  $\Gamma_L = \Gamma_R = \Gamma/2$ ,  $\omega_L = 0.5\epsilon_0$ ,  $J = 0.01\epsilon_0$ ,  $S = 100$ . Grid lines for  $\theta = \pi/3$  (green line), are positioned at  $D = -0.01312\epsilon_0$  ( $\mu_L = \epsilon_2$ ),  $D = -0.00625\epsilon_0$  ( $\mu_R = \epsilon_3$ ),  $D = 0.00875\epsilon_0$  ( $\mu_R = \epsilon_4$ ), and  $D = 0.01406\epsilon_0$  ( $\mu_L = \epsilon_1$ ).

pendix]. On the other hand, for  $\theta = \pi/2$ , the molecular spin is perpendicular to  $z$ -axis,  $S_z = 0$ , and  $\alpha$ ,  $\beta$ ,  $T_{\perp}$  and  $T_z$  are independent of  $D$ . Here,  $\alpha$ ,  $T_{\perp}$  and  $T_z$  vanish, while  $\beta$  takes a negative constant value (pink dashed lines in Fig. 4). According to the second term in Eq. (23) the torque with negative  $\beta$  tends to change the direction of the molecular spin precession. Grid lines in Fig. 4 are related to  $\theta = \pi/3$ ,  $\omega_L = 0.5\epsilon_0$  (green lines) and the values of parameter  $D$ , such that  $\mu_L$  or  $\mu_R$  is in resonance with one of the four quasienergy levels  $\epsilon_i$ . Around  $D = -0.01312\epsilon_0$  corresponding to  $\mu_L = \epsilon_2$  (the first grid line from the left), one notices a small local maximum in  $\alpha$ , a local minimum in  $\beta$ , a local maximum in  $T_{\perp}$ , while  $T_z$  has a minimum negative value. For this set of parameters, levels  $\epsilon_1$  (spin-down),  $\epsilon_2$  (spin-up) and  $\epsilon_4$  (spin-up) lie within the bias-voltage window, while  $\epsilon_3$  (spin-down) is below  $\mu_R$ . This means that there are more inelastic tunnelling pathways, involving electron spin-flip, available for spin-down electrons than for spin-up electrons. Namely, a tunneling spin-down electron in the level  $\epsilon_3$

can flip its spin and enter the spin-up level  $\epsilon_4$  within the bias voltage window, before it tunnels off the orbital, but the spin-up electron from the level  $\epsilon_4$  cannot flip its spin and enter spin-down level  $\epsilon_3$ , since  $\epsilon_3$  lies below the bias voltage window. As a consequence, more spin-down electrons participate in inelastic spin transport, resulting in the negative torque component  $T_z$ . With further increase of the anisotropy parameter  $D$ , for  $\theta = \pi/3$  and  $\omega_L = 0.5\epsilon_0$ , the torque  $T_z$  remains negative until around  $D = -0.00625\epsilon_0$  corresponding to  $\mu_R = \epsilon_3$ , depending on the level broadening  $\Gamma$  (second grid line from the left). Here, the torque  $T_z$  has another local negative minimum and a step-like increase towards zero, while the Gilbert damping coefficient  $\alpha$  has a local maximum and a step-like decrease towards zero, which means that  $T_z$  and  $\alpha$  vanish when all four levels lie within the bias-voltage window, with respect to the broadening  $\Gamma$ . On the other hand,  $T_{\perp}$  has a maximum value when all the levels  $\epsilon_i$  lie within the bias-voltage window at  $D = -0.00625\epsilon_0$ , while the coefficient  $\beta$  has another local minimum. As



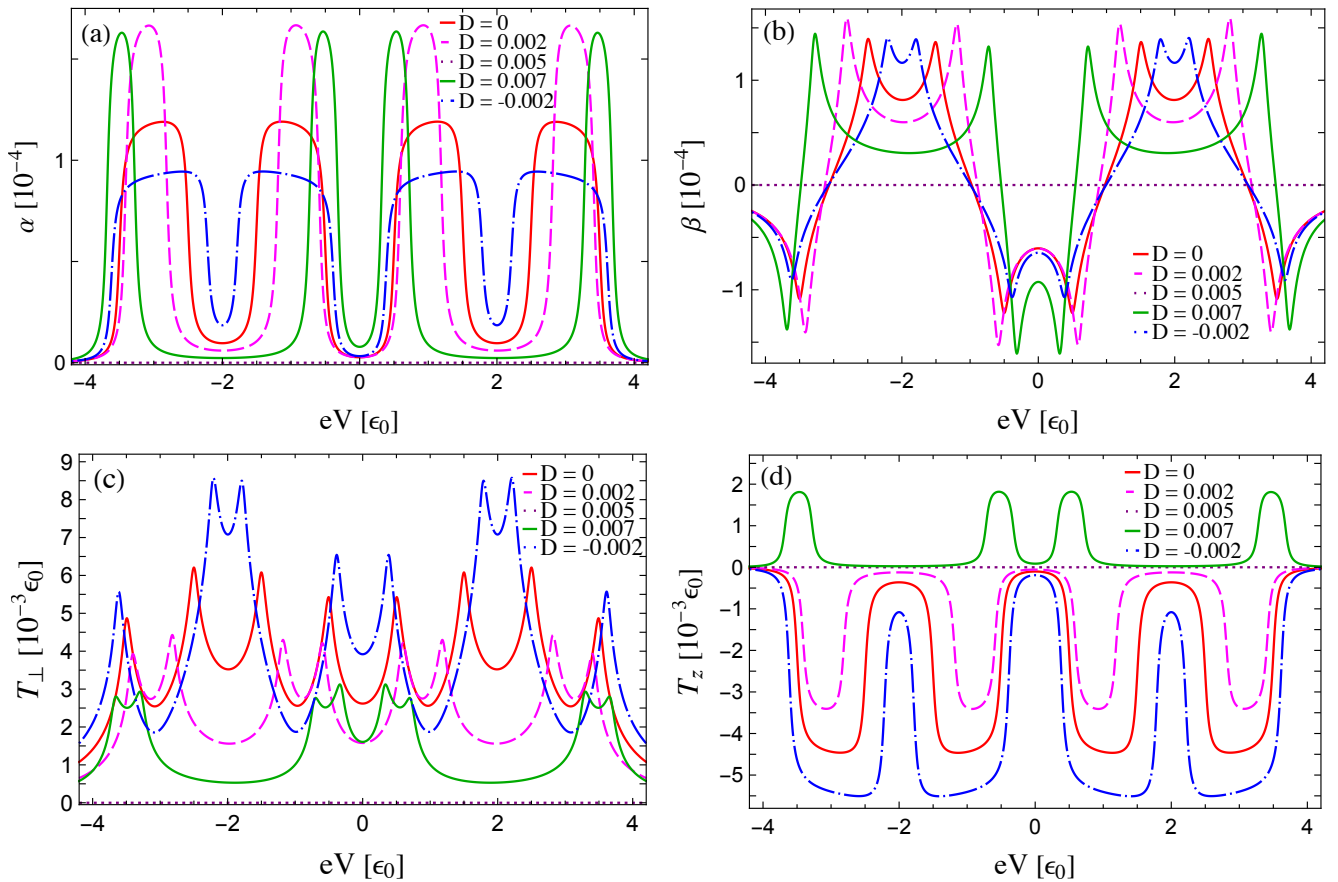


FIG. 5: (Color online) (a) Gilbert damping coefficient  $\alpha$ , (b) coefficient  $\beta$ , (c) magnitude of the in-plane component of the spin-transfer torque,  $T_{\perp}$  and (d) spatial component of the torque along  $z$ -direction  $T_z$ , as functions of the applied bias voltage  $eV = \mu_L - \mu_R$  with  $\mu_{L,R} = \pm eV/2$  and  $\vec{B} = B\vec{e}_z$ , for different uniaxial magnetic anisotropy parameters  $D$  at zero temperature. The other parameters are set to:  $\Gamma = 0.05 \epsilon_0$ ,  $\Gamma_L = \Gamma_R = \Gamma/2$ ,  $\omega_L = 0.5 \epsilon_0$ ,  $J = 0.01 \epsilon_0$ ,  $S = 100$ , and  $\theta = \pi/3$ . All energies are given in the units of  $\epsilon_0$ . For  $D = \omega_L/2S_z = 0.005 \epsilon_0$ ,  $\alpha = 0$ ,  $\beta = 0$ , and  $\vec{T} = 0$  (purple dotted lines).

the increase of the anisotropy parameter  $D$  continues, the Gilbert damping coefficient  $\alpha$  and  $T_z$  remain zero until around  $D = 0.00875 \epsilon_0$ , corresponding to  $\mu_R = \epsilon_4$  (third grid line from the left). Here,  $\alpha$  reaches its maximum value, while  $\vec{T}_z$  changes its direction and has a step-like increase towards a local maximum, the coefficient  $\beta$  has its minimum value, while  $T_{\perp}$  has a local maximum. With further increase of  $D$ , since levels  $\epsilon_1$ ,  $\epsilon_2$  and  $\epsilon_3$  lie within the bias-voltage window, while the spin-up level  $\epsilon_4$  goes below,  $\epsilon_4 < \mu_R$ , with  $\epsilon_3 > \epsilon_4$  for  $\omega < 0$ , there are more inelastic tunnelling pathways available for spin-up particles. Hence, the resulting torque component  $T_z > 0$ . Around  $D = 0.01406 \epsilon_0$ , corresponding to  $\mu_L = \epsilon_1$ , the coefficient  $\alpha$ , the magnitude of the in-plane torque component,  $T_{\perp}$ , and  $T_z$  have a local maximum (the fourth grid line from the left), while  $\beta$  has a local minimum for  $\theta = \pi/3$  and  $\omega_L = 0.5 \epsilon_0$ . Note that the in-plane torque  $T_{\perp}$  decreases from its maximum value to zero in the region  $-0.00625 \epsilon_0 < D < 0.005 \epsilon_0$ , where  $\omega > 0$ , and increases for  $0.005 \epsilon_0 < D < 0.00875 \epsilon_0$ , where  $\omega < 0$  [see green line in Fig. 4(c)]. At  $D = 0.005 \epsilon_0$ , for  $\theta = \pi/3$  and

$\omega_L = 0.5 \epsilon_0$ , the total frequency  $\omega = \omega_L - 2DS_z = 0$ , and the direction of the precession changes, while  $T_{\perp} = 0$ . In the absence of the magnetic field, with  $\omega_L = 0$ , for  $\theta = \pi/3$ , the torque component  $T_{\perp} = 0$  at  $D = 0$  [orange line in Fig. 4(c)]. Similarly, for  $\theta = \pi/9$  and  $\theta = \pi/4$  [red and blue dot-dashed lines in Fig. 4(c)], the torque  $T_{\perp} = 0$  for  $\omega_L = 2DS_z$ , while  $\alpha$  and  $T_z$  go to zero for the values of  $D$  such that each  $\epsilon_i$  satisfies  $\mu_R \leq \epsilon_i \leq \mu_L$ , with respect to level broadening  $\Gamma$ . In Fig. 4,  $\alpha$ ,  $\beta$ ,  $T_{\perp}$  and  $T_z$  vanish for a very large  $|D|$ , except for  $\theta = 0, \pi/2$ .

The torque coefficients  $\alpha$  and  $\beta$ , the magnitude of the in-plane torque component,  $T_{\perp}$ , and  $z$ -component of the spin-transfer torque,  $T_z$ , as functions of the applied bias-voltage  $eV$  are presented in Fig. 5 for several different magnetic anisotropy parameters  $D$  at zero temperature. The bias voltage is varied according to  $\mu_{L,R} = \pm eV/2$ . For the anisotropy parameter  $D = \omega_L/2S_z = 0.005 \epsilon_0$ , the molecular spin is static,  $\omega = 0$ , and only elastic spin transport occurs through two available transport channels, so that the spin-transfer torque and the torque coefficients  $\alpha$  and  $\beta$  vanish (purple dotted lines in Fig. 5).

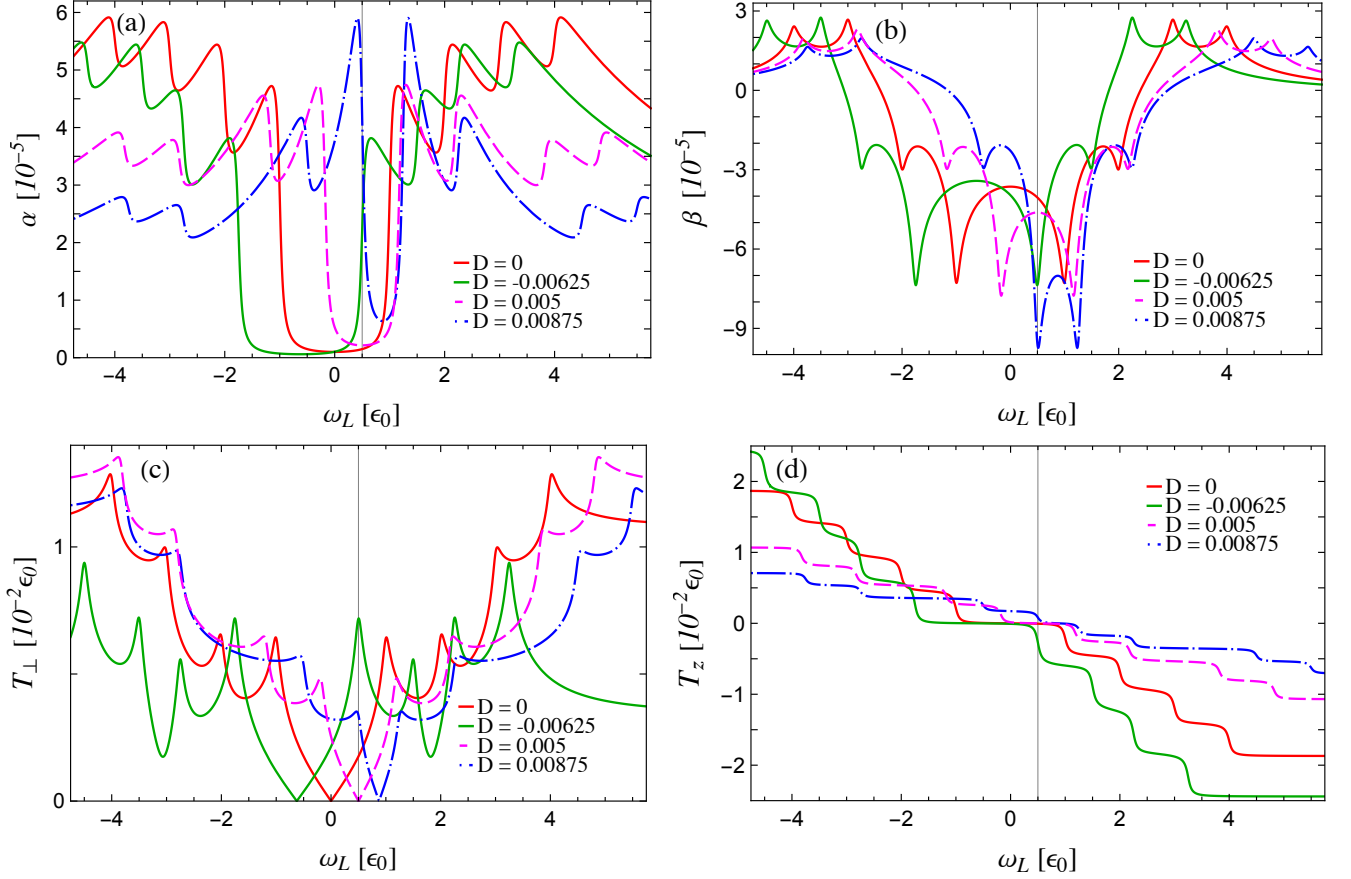


FIG. 6: (Color online) (a) Gilbert damping coefficient  $\alpha$ , (b) coefficient  $\beta$ , (c) magnitude of the in-plane component of the spin-transfer torque,  $T_{\perp}$  and (d) spatial component of the torque along  $z$ -direction  $T_z$ , as functions of the Larmor frequency  $\omega_L$  for different uniaxial magnetic anisotropy parameters  $D$ . All plots are obtained at zero temperature with  $\vec{B} = B\vec{e}_z$ . The chemical potentials of the leads are equal to:  $\mu_R = 0$  and  $\mu_L = 2.5\epsilon_0$ . The other parameters are set to:  $\Gamma = 0.05\epsilon_0$ ,  $\Gamma_L = \Gamma_R = \Gamma/2$ ,  $J = 0.01\epsilon_0$ ,  $S = 100$ , and  $\theta = \pi/3$ . All energies are given in the units of  $\epsilon_0$ . For a suppressed precession, with  $\omega = 0$ ,  $\omega_L = 2DS_z$ , the spin-transfer torque vanishes,  $T_{\perp} = 0$  and  $T_z = 0$  (intersection between grid line and pink dashed line).

For  $D \neq 0.005\epsilon_0$ , starting with  $eV = 0$  and increasing the bias voltage, we notice that  $\alpha$  and the magnitude of the spatial  $z$ -component of the torque  $|T_z|$ , are increased for chemical potentials  $\mu_{\xi}$  between quasienergy levels  $\epsilon_i$  connected with a spin-flip, where they approach constant values. For  $\omega > 0$ , i.e.,  $D < \omega_L/2S_z$ , with the increase of  $D$ , these values of  $\alpha$  increase, whereas  $|T_z|$  decrease [blue dot-dashed, red, and pink dashed lines in Figs. 5(a) and 5(d)], whereas they drop to zero for  $\omega = 0$  as already mentioned, and arise again for  $\omega < 0$ , i.e.,  $D > \omega_L/2S_z$  [green lines in Figs. 5(a) and 5(d)]. Moreover, the position of the bias-voltage window where the inelastic transport events occur and its width  $w = 2\omega = 2\omega_L - 4DS_z$  change with the change of  $D$ , taking into account the level broadening  $\Gamma$ . Note that  $T_z > 0$  for  $D < \omega_L/2S_z$ , and  $T_z < 0$  for  $D > \omega_L/2S_z$ . In the same regions, the coefficient  $\beta$  increases(decreases) from a local minimum(maximum) to a local maximum(minimum), causing the torque  $\beta\vec{S}$  to oppose(enhance) the rotational motion of the molecular spin  $\vec{S}$ , for negative(positive)  $\beta$ .

All peaks in  $T_{\perp}$  correspond to  $\mu_{\xi} = \epsilon_i$ . Their values decrease with the increase of  $D$  for  $\omega > 0$  [blue dot-dashed, red, and pink dashed lines in Fig. 5(c)], drop to zero for  $\omega = 0$ , and arise again for  $\omega < 0$ . For the values of bias voltage  $eV$  such that  $\beta = 0$ , while  $\alpha$  and  $|T_z|$  approach their maximums, the magnitude  $T_{\perp}$  has local minimums. For large values of  $|D|$ , the spin torque coefficients and spatial components of the spin-transfer torque vanish as functions of the bias voltage  $eV$ .

In Fig. 6 the Gilbert damping coefficient  $\alpha$ , the coefficient  $\beta$ , the magnitude of the in-plane spin-transfer torque component,  $T_{\perp}$  and the spin-transfer torque along the  $z$ -direction,  $T_z$ , are plotted as functions of the Larmor frequency  $\omega_L$  at zero temperature, for four different values of the uniaxial magnetic anisotropy parameter  $D$ . The bias voltage is varied as  $eV = \mu_L - \mu_R$ , with  $\mu_L = 2.5\epsilon_0$  and  $\mu_R = 0$ . The positions and values of all the local maximums in  $\alpha$  and steps in  $T_z$ , peaks and dips in  $\beta$ , and peaks in  $T_{\perp}$  depend on the magnetic anisotropy parameter  $D$ . They correspond to a reso-

nance between  $\mu_\xi$  and the level with energy  $\epsilon_i$ , available for spin-transport,  $\mu_\xi = \epsilon_i$ , denoting inelastic tunnelling processes, each involving a spin-flip accompanied by absorption(emission) of an energy  $\omega$ . For the anisotropic molecular spin, the Gilbert damping coefficient  $\alpha$ , the coefficient  $\beta$  and the magnitude of the in-plane torque component  $T_\perp$  are even functions, while spin-transfer torque component  $T_z$  is an odd function of  $\omega$ . Hence, for the isotropic molecular spin ( $D = 0$ ), the torque coefficients  $\alpha(\omega_L) = \alpha(-\omega_L)$  and  $\beta(\omega_L) = \beta(-\omega_L)$ ,<sup>88</sup> whereas  $T_\perp(\omega_L) = T_\perp(-\omega_L)$  and  $T_z(\omega_L) = -T_z(-\omega_L)$ . Around  $\omega_L = 0.5 \epsilon_0$  (vertical grid lines in Fig. 6) a maximum value for  $D = 0.00875 \epsilon_0$  and a local maximum for  $D = -0.00625 \epsilon_0$  can be observed in  $\alpha$  due to resonances  $\mu_R = \epsilon_4$  and  $\mu_R = \epsilon_3$ , while the coefficient  $\beta$  shows negative minimums,  $T_\perp$  local maximums, and  $T_z$  step-like decreases [blue dot-dashed and green lines in Fig. 6]. Looking at positive Larmor frequency  $\omega_L > 0$  for  $D = -0.00625 \epsilon_0$  (green lines in Fig. 6), one notices that for  $\omega_L < 0.5 \epsilon_0$  all four quasienergy levels  $\epsilon_i$  lie within the bias-voltage window. With the increase of  $\omega_L$  they leave the bias-voltage window one after the other after reaching a resonance with  $\mu_R$  or  $\mu_L$ :  $\epsilon_3 = \mu_R$  at  $\omega_L = 0.5 \epsilon_0$  (grid line corresponding to the grid line in Fig. 4),  $\epsilon_2 = \mu_L$  at  $\omega_L = 1.5 \epsilon_0$ ,  $\epsilon_1 = \mu_R$  at  $\omega_L = 2.25 \epsilon_0$ , and  $\epsilon_4 = \mu_L$  at  $\omega_L = 3.25 \epsilon_0$ . If we take into account the level broadening  $\Gamma$ , all four quasienergy levels  $\epsilon_i$  leave the bias-voltage window around  $\omega_L = 3.25 \epsilon_0$ , with spin-up levels  $\epsilon_{2(4)} > \mu_L$ , and spin-down levels  $\epsilon_{1(3)} < \mu_R$ . With further increase of  $\omega_L$ ,  $\alpha$  and  $\beta$  vanish, while  $T_\perp$  and  $T_z$  become saturated due to inelastic spin-flip processes involving spin particles from the leads entering spin-down levels with energies  $\epsilon_1$  or  $\epsilon_3$ , flipping their spin and returning back to the leads with absorbed energy  $\omega$  after the interaction with the molecular spin  $\vec{S}$  (note that saturated  $T_z < 0$  for  $\omega_L > 0$ ). For the uniaxial magnetic anisotropy parameter  $D = \omega_L/2S_z$ , e.g., for  $D = 0.005 \epsilon_0$  at  $\omega_L = 0.5 \epsilon_0$ , the frequency  $\omega = 0$  and spin-transfer torque components vanish,  $T_\perp = 0$  and  $T_z = 0$ , since the molecular spin  $\vec{S}$  is static in this case [intersection between grid line and pink-dashed line in Figs. 6(c) and 6(d)]. Also, for large values of  $|D|$ , the Gilbert damping coefficient  $\alpha$  and the coefficient  $\beta$ , as well as  $T_\perp$  and  $T_z$  vanish as functions of the Larmor frequency  $\omega_L$ .

## V. CONCLUSIONS

In this paper, the properties of spin transport through a junction consisting of a single orbital of a magnetic molecule with precessing anisotropic spin in a constant magnetic field was theoretically studied. The orbital is connected to two Fermi leads. The precession is kept undamped by external means and the precession frequency involves two contributions, one is Larmor frequency and the other is a term involving the uniaxial magnetic anisotropy parameter. Using the Keldysh NEGF technique, the spin currents, noise of  $z$ -polarized

spin current, spin-transfer torque with the Gilbert damping coefficient and other torque coefficients were derived.

The results were discussed and analysed at zero temperature. The observed spin-transport characteristics such as steps, peaks and dips are related to resonances between chemical potentials of the leads and molecular quasienergy levels which depend on the uniaxial magnetic anisotropy parameter of the molecular spin. The inelastic tunnelling of an electron spin that involves a spin-flip and absorption(emission) of an energy that depends on the magnetic anisotropy occurs due to exchange interaction with the precessing anisotropic molecular spin. During that process, the spin-transfer torque is exerted on the spin of the molecule. Both torque coefficients  $\alpha$  and  $\beta$ , as well as the magnitude of the in-plane torque  $T_\perp$  are even functions, while  $T_z$  is an odd function of the total precession frequency, taking into consideration the contribution of the magnetic anisotropy to the precession.

By adjusting the uniaxial magnetic anisotropy parameter with respect to the Larmor precession frequency and the tilt angle between the magnetic field and the molecular spin, one can control the spin current and noise, the spin-transfer torque, the Gilbert damping and the other torque coefficients. Furthermore, it might be possible to perform a measurement of the dc-spin current and spin-transfer torque components, since they reveal the quasienergy level structure in the molecular orbital and all spatial components of the spin-transfer torque vanish for the anisotropy contribution to the precession frequency that matches the Larmor frequency, when the precession is suppressed, thus allowing to determine the anisotropy and other parameters. Also, large uniaxial anisotropy parameter leads to vanishing of the spin current and spin-current noise, spin-transfer torque, as well as the corresponding torque coefficients.

Taking into account that the spin currents and corresponding noise and magnitude, direction and sign of the spin-transfer torque can be manipulated by the uniaxial magnetic anisotropy and other parameters, even without applied magnetic field is turned off, the obtained results might be useful in spintronic applications using molecular magnets. Since magnetic anisotropy parameter is important for applications of molecular magnets in magnetic storage, it might be suitable to study noise of spin-transfer torque to obtain additional characteristics of spin-transport, and use quantum-mechanical description of the anisotropic molecular spin in tunnel junctions with normal or ferromagnetic leads.

## Acknowledgments

The author acknowledges funding provided by the Institute of Physics Belgrade, through the grant No: 451-03-68/2022-14/200024 of the Ministry of Education, Science, and Technological Development of the Republic of Serbia.

### Appendix: Expressions for the components of spin current

The expressions for complex functions  $I_{\xi x}(D)$  and  $I_{\xi y}(D)$  introduced by Eq. (7) and Eq. (8), and spin-current component  $I_{\xi z}$ , are presented here in terms of the Green's functions  $\hat{G}^{0r}(\epsilon)$  and  $\hat{G}^{0a}(\epsilon) = [\hat{G}^{0r}(\epsilon)]^\dagger$ . They can be written as

$$I_{\xi x}(D) = -i \int \frac{d\epsilon}{4\pi} \left\{ \frac{\Gamma_\xi \Gamma_\eta}{\Gamma} [f_\xi(\epsilon) - f_\eta(\epsilon)] \left[ \frac{\gamma G_{11}^{0r}(\epsilon + \omega_L - 2DS_z) G_{22}^{0r}(\epsilon)}{|1 - \gamma^2 G_{11}^{0r}(\epsilon + \omega_L - 2DS_z) G_{22}^{0r}(\epsilon)|^2} \right. \right. \\ \left. \left. + \frac{2i\gamma \text{Im}\{G_{11}^{0r}(\epsilon)\} G_{22}^{0a}(\epsilon - \omega_L + 2DS_z) + \gamma^3 |G_{11}^{0r}(\epsilon) G_{22}^{0r}(\epsilon - \omega_L + 2DS_z)|^2}{|1 - \gamma^2 G_{11}^{0r}(\epsilon) G_{22}^{0r}(\epsilon - \omega_L + 2DS_z)|^2} \right] \right. \\ \left. + \sum_{\lambda, \zeta=L,R} \frac{\Gamma_\lambda \Gamma_\zeta}{\Gamma} [f_\lambda(\epsilon - \omega_L + 2DS_z) - f_\zeta(\epsilon)] \right. \\ \left. \times \left[ \delta_{\zeta\xi} - \delta_{\lambda\xi} \gamma^2 G_{11}^{0a}(\epsilon) G_{22}^{0r}(\epsilon - \omega_L + 2DS_z) \right] \frac{\gamma G_{11}^{0r}(\epsilon) G_{22}^{0a}(\epsilon - \omega_L + 2DS_z)}{|1 - \gamma^2 G_{11}^{0r}(\epsilon) G_{22}^{0r}(\epsilon - \omega_L + 2DS_z)|^2} \right\}, \quad \eta \neq \xi, \quad (\text{A1})$$

$$I_{\xi y}(D) = iI_{\xi x}(D), \quad (\text{A2})$$

$$\text{and } I_{\xi z} = \int \frac{d\epsilon}{4\pi} \left\{ \frac{\Gamma_\xi \Gamma_\eta}{\Gamma} [f_\xi(\epsilon) - f_\eta(\epsilon)] \left[ \frac{2\text{Im}\{G_{11}^{0r}(\epsilon)\}}{|1 - \gamma^2 G_{11}^{0r}(\epsilon) G_{22}^{0r}(\epsilon - \omega_L + 2DS_z)|^2} - \frac{2\text{Im}\{G_{22}^{0r}(\epsilon)\}}{|1 - \gamma^2 G_{11}^{0r}(\epsilon + \omega_L - 2DS_z) G_{22}^{0r}(\epsilon)|^2} \right] \right. \\ \left. + \sum_{\lambda, \zeta=L,R} \Gamma_\lambda \Gamma_\zeta [f_\lambda(\epsilon - \omega_L + 2DS_z) - f_\zeta(\epsilon)] (\delta_{\lambda\xi} + \delta_{\zeta\xi}) \frac{\gamma^2 |G_{11}^{0r}(\epsilon) G_{22}^{0r}(\epsilon - \omega_L + 2DS_z)|^2}{|1 - \gamma^2 G_{11}^{0r}(\epsilon) G_{22}^{0r}(\epsilon - \omega_L + 2DS_z)|^2} \right\}, \quad \eta \neq \xi. \quad (\text{A3})$$

- 
- <sup>1</sup> L. Thomas, F. Lioni, R. Ballou, D. Gatteschi, R. Sessoli, and B. Barbara, *Nature* **383**, 145-147 (1996).
- <sup>2</sup> D. Gatteschi, R. Sessoli, and J. Villain, *Molecular Nanomagnets*, Oxford University Press, New York (2006).
- <sup>3</sup> L. Bogani and W. Wernsdorfer, *Nature Mater.* **7**, 179-186 (2008).
- <sup>4</sup> C. Timm and M. Di Ventura, *Phys. Rev B* **86**, 104427 (2012).
- <sup>5</sup> M. N. Leuenberger and D. Loss, *Nature* **410**, 789-793 (2001).
- <sup>6</sup> R. E. P. Winpenny, *Angew. Chem. Int. Ed.*, **47**, 7992-7994 (2008).
- <sup>7</sup> M. -H. Jo, J. E. Grose, K. Baheti, M. M. Deshmukh, J. J. Sokol, E. M. Rumberger, D. N. Hendrickson, J. R. Long, H. Park, and D. C. Ralph, *Nano Lett.* **6**, 2014 (2006).
- <sup>8</sup> A. S. Zyazin, J. W. G. van den Berg, E. A. Osorio, H. S. J. van der Zant, N. P. Konstantinidis, M. Leijnse, M. R. Wegewijs, F. May, W. Hofstetter, C. Danieli, and A. Cornia, *Nano Lett.* **10**, 3307 (2010).
- <sup>9</sup> E. Burzurí, A. S. Zyazin, A. Cornia, and H. S. J. van der Zant, *Phys. Rev. Lett.* **109**, 147203 (2012).
- <sup>10</sup> M. Misiorny, M. Hell, and M. R. Wegewijs, *Nature Physics* **9**, 801-805 (2013).
- <sup>11</sup> H. B. Heersche, Z. de Groot, J. A. Folk, H. S. J. van der Zant, C. Romeike, M.R. Wegewijs, L. Zobbi, D. Barreca, E. Tondello, and A. Cornia, *Phys. Rev. Lett.* **96**, 206801 (2006).
- <sup>12</sup> R. Sessoli, *Nature* **548**, 400-401 (2017).
- <sup>13</sup> F. Delgado and J. Fernández-Rossier, *Phys. Rev. Lett.* **108**, 196602 (2012).
- <sup>14</sup> S. Kahle, Z. Deng, N. Malinowski, C. Tonnoir, A. Forment-Aliaga, N. Thontasen, G. Rinke, D. Le, V. Turkowski, T. S. Rahman, S. Rauschenbach, M. Ternes, and K. Kern, *Nano Lett.* **12**, 518-521 (2012).
- <sup>15</sup> F. -S. Guo, B. M. Day, Y. -C. Chen, M. -L. Tong, A. Mansikkamäki, and R. A. Layfield, *Science* **362**, 1400-1403 (2018).
- <sup>16</sup> R. Sessoli, D. Gatteschi, A. Caneschi, and M. A. Novak, *Nature* **365** 141-143 (1993).
- <sup>17</sup> M. Misiorny and J. Barnaś, *Phys. Rev. B* **77**, 172414 (2008).
- <sup>18</sup> Y. Shiota, T. Nozaki, F. Bonell, S. Murakami, T. Shinjo, and Y. Suzuki, *Nature Mater.* **11**, 39-43 (2012).
- <sup>19</sup> B. W. Heinrich, L. Braun, J. I. Pascual, K. J. Franke, *Nano Lett.* **15**, 4024-4028 (2015).
- <sup>20</sup> J. D. V. Jaramillo, H. Hammar, and J. Fransson, *ACS Omega* **3**, 6546-6553 (2018).
- <sup>21</sup> B. Rana and Y. Otani, *Commun. Phys.* **2**, 90 (2019).
- <sup>22</sup> R. E. George, J. P. Edwards, and A. Ardavan, *Phys. Rev. Lett.* **110**, 027601 (2013).
- <sup>23</sup> A. Sarkar and G. Rajaraman, *Chem. Sci.* **11**, 10324-10330 (2020).

- <sup>24</sup> Y. Lu, Y. Wang, L. Zhu, L. Yang, and L. Wang, *Phys. Rev. B* **106**, 064405 (2022).
- <sup>25</sup> M. Pletyukhov, D. Schuricht, and H. Schoeller, *Phys. Rev. Lett.* **104**, 106801 (2010).
- <sup>26</sup> R. Wieser, *Phys. Rev. Lett.* **110**, 147201 (2013).
- <sup>27</sup> R. Mondal, M. Berritta, and P. M. Oppeneer, *Phys. Rev. B* **94**, 144419 (2016).
- <sup>28</sup> M. Sayad, R. Rausch, and M. Potthoff, *Phys. Rev. Lett.* **117**, 127201 (2016).
- <sup>29</sup> A. Barman, S. Mandal, S. Sahoo, and A. De, *J. Appl. Phys.* **128**, 170901 (2020).
- <sup>30</sup> L. Yang, P. Glasenapp, A. Greilich, D. Reuter, A. D. Wieck, D. R. Yakovlev, M. Bayer, and S. A. Crooker, *Nat. Commun.* **5**, 4949 (2014).
- <sup>31</sup> W. D. Rice, W. Liu, T. A. Baker, N. A. Sinitsyn, V. I. Klimov, and S. A. Crooker, *Nat. Nanotechnol.* **11**, 137-142 (2016).
- <sup>32</sup> M. Swar, D. Roy, S. Bhar, S. Roy, and S. Chaudhuri, *Phys. Rev. Res.* **3**, 043171 (2021).
- <sup>33</sup> C. Stahl and M. Potthoff, *Phys. Rev. Lett.* **119**, 227203 (2017).
- <sup>34</sup> U. Bajpai and B. K. Nikolić, *Phys. Rev. Lett.* **125**, 187202 (2020).
- <sup>35</sup> P. M. Gunnink, T. Ludwig, and R. A. Duine, *Phys. Rev. B* **109**, 024408 (2024).
- <sup>36</sup> D. C. Ralph and M. D. Stiles, *J. Magn. Magn. Mater.* **320**, 1190-1216 (2008).
- <sup>37</sup> J. -X. Zhu, Z. Nussinov, A. Shnirman, and A. V. Balatsky, *Phys. Rev. Lett.* **92**, 107001 (2004).
- <sup>38</sup> Z. Nussinov, A. Shnirman, D. P. Arovas, A. V. Blaltsky, and J. -X. Zhu, *Phys. Rev. B* **71**, 214520 (2005).
- <sup>39</sup> J. -X. Zhu and J. Fransson, *J. Phys.: Condens. Matter* **18**, 9929-9936 (2006).
- <sup>40</sup> J. Fransson and J. -X. Zhu, *New J. Phys.* **10**, 013017 (2008).
- <sup>41</sup> Jonas Fransson, *Phys. Rev. B* **77**, 205316 (2008).
- <sup>42</sup> J. Fransson, J. Ren, and J. X. Zhu, *Phys. Rev. Lett.* **113**, 257201 (2014).
- <sup>43</sup> H. Hammar and J. Fransson, *Phys. Rev. B* **94**, 054311 (2016).
- <sup>44</sup> H. Hammar and J. Fransson, *Phys. Rev. B* **96**, 214401 (2017).
- <sup>45</sup> H. Hammar and J. Fransson, *Phys. Rev. B* **98**, 174438 (2018).
- <sup>46</sup> H. Hammar, J. D. V. Jaramillo, and J. Fransson, *Phys. Rev. B* **99**, 115416 (2019).
- <sup>47</sup> I. Makhfudz, E. Olive, and S. Nicolis, *Appl. Phys. Lett.* **117**, 132403 (2020).
- <sup>48</sup> R. Rahman and S. Bandyopadhyay, *J. Phys.: Condens. Matter* **33**, 355801 (2021).
- <sup>49</sup> J. C. Slonczewski, *J. Magn. Magn. Mater.* **159**, L1-L7 (1996).
- <sup>50</sup> L. Berger, *Phys. Rev. B* **54**, 9353-9358 (1996).
- <sup>51</sup> M. Tsoi, A. G. M. Jansen, J. Bass, W. -C. Chiang, M. Seck, V. Tsoi and P. Wyder, *Phys. Rev. Lett.* **80**, 4281 (1998).
- <sup>52</sup> J. Z. Sun, *J. Magn. Magn. Mater.* **202**, 157-162 (1999).
- <sup>53</sup> Y. Tserkovnyak, A. Brataas, and G. E. W. Bauer, *Phys. Rev. B* **66**, 224403 (2002).
- <sup>54</sup> G. E. W. Bauer, E. Saitoh, and B. J. van Wees, *Nature Mater.* **11**, 391 (2012).
- <sup>55</sup> E. B. Myers, D. C. Ralph, J. A. Katine, R. N. Louie, and R. A. Buhrman, *Science* **285**, 867-870 (1999).
- <sup>56</sup> F. J. Albert, N. C. Emley, E. B. Myers, D. C. Ralph, and R. A. Buhrman, *Phys. Rev. Lett.* **89**, 226802 (2002).
- <sup>57</sup> S. I. Kiselev, J. C. Sankey, I. N. Krivorotov, N. C. Emley, R. J. Schoelkopf, R. A. Buhrman, and D. C. Ralph, *Nature* **425**, 380-383 (2003).
- <sup>58</sup> L. Liu, C. -F. Pai, Y. Li, H. W. Tseng, D. C. Ralph, and R. A. Buhrman, *Science* **336**, 555-558 (2012).
- <sup>59</sup> A. Chudnovskiy, Ch. Hübner, B. Baxevanis, and D. Pfannkuche, *Phys. Status Solidi B*, 251, 1764 (2014).
- <sup>60</sup> T. Ludwig, I. S. Burmistrov, Y. Gefen, and A. Shnirman, *Phys. Rev. B* **95**, 075425 (2017).
- <sup>61</sup> M. Misiorny and J. Barnaś, *Phys. Rev. B* **75**, 134425 (2007).
- <sup>62</sup> M. Misiorny and J. Barnaś, *Phys. Rev. Lett.* **111**, 046603 (2013).
- <sup>63</sup> K. Wrześniewski and I. Weymann, *Phys. Rev. B* **101**, 245434 (2020).
- <sup>64</sup> H. -B. Xue, J. -Q. Liang and W. -M. Liu, *Physica E* **138**, 115086 (2022).
- <sup>65</sup> C. Timm and F. Elste, *Phys. Rev. B* **73**, 235304 (2006).
- <sup>66</sup> K. Xia, P. J. Kelly, G. E. W. Bauer, A. Brataas, and I. Turek, *Phys. Rev. B* **65**, 220401(R) (2002).
- <sup>67</sup> Y. Tserkovnyak, A. Brataas, G. E. E. Bauer, and B. I. Halperin, *Rev. Mod. Phys.* **77**, 1375 (2005).
- <sup>68</sup> E. M. Hankiewicz, G. Vignale, and Y. Tserkovnyak, *Phys. Rev. B* **75**, 174434 (2007).
- <sup>69</sup> E. M. Hankiewicz, G. Vignale, and Y. Tserkovnyak, *Phys. Rev. B* **78**, 020404(R) (2008).
- <sup>70</sup> Y. Tserkovnyak, E. M. Hankiewicz, and G. Vignale, *Phys. Rev. B* **79**, 094415 (2009).
- <sup>71</sup> G. Tatara, H. Kohno, and J. Shibata, *Phys. Rep.* **468**, 213 (2008).
- <sup>72</sup> G. Tatara, *Physica E* **106**, 208 (2019).
- <sup>73</sup> C. Bell, S. Milikisyants, M. Huber, and J. Aarts, *Phys. Rev. Lett.* **100**, 047002 (2008).
- <sup>74</sup> M. Houzet, *Phys. Rev. Lett.* **101**, 057009 (2008).
- <sup>75</sup> J. P. Morten, A. Brataas, G. E. W. Bauer, W. Belzig, and Y. Tserkovnyak, *EPL* **84**, 57008 (2008).
- <sup>76</sup> S. Teber, C. Holmqvist, and M. Fogelstör, *Phys. Rev. B* **81**, 174503 (2010).
- <sup>77</sup> C. Holmqvist, M. Fogelstör, and W. Belzig, *Phys. Rev. B* **90**, 014516 (2014).
- <sup>78</sup> Y. Yao, Q. Song, Y. Takamura, J. P. Cascales, W. Yuan, Y. Ma, Y. Yun, X. C. Xie, J. S. Moodera, and W. Han, *Phys. Rev. B* **97**, 224414 (2018).
- <sup>79</sup> T. Kato, Y. Ohnuma, M. Matsuo, J. Rech, T. Jonckheere, and T. Martin, *Phys. Rev. B* **99**, 144411 (2019).
- <sup>80</sup> N. S. Wingreen, A.-P. Jauho, and Y. Meir, *Phys. Rev. B* **48**, 8487 (1993).
- <sup>81</sup> A.-P. Jauho, N. S. Wingreen, and Y. Meir, *Phys. Rev. B* **50**, 5528 (1994).
- <sup>82</sup> A.-P. Jauho and H. Haug, *Quantum Kinetics in Transport and Optics of Semiconductors* (Springer, Berlin, 2008).

- <sup>83</sup> Q.-f. Sun, H. Guo, and J. Wang, Phys. Rev. Lett. **90**, 258301 (2003).
- <sup>84</sup> J. Fransson and M. Galperin, Phys. Rev. B **81**, 075311 (2010).
- <sup>85</sup> A. Saraiva-Souza, M. Smeu, L. Zhang, A. G. Souza Filho, H. Guo, and M. A. Ratner, J. Am. Chem. Soc. **136**, 42, 15065-15071 (2014).
- <sup>86</sup> J. Fransson, O. Eriksson, and A. V. Balatsky, Phys. Rev. B **81**, 115454 (2010).
- <sup>87</sup> D. Rai and M. Galperin, Phys. Rev. B **86**, 045420 (2012).
- <sup>88</sup> M. Filipović, C. Holmqvist, F. Haupt, and W. Belzig, Phys. Rev. B **87**, 045426 (2013); **88**, 119901 (2013).
- <sup>89</sup> M. Filipović and W. Belzig, Phys. Rev. B **93**, 075402 (2016).
- <sup>90</sup> S. Lounis, A. Bringer, and S. Blügel, Phys. Rev. Lett. **108**, 207202 (2012).
- <sup>91</sup> D. Yudin, D. R. Gulevich, and M. Titov, Phys. Rev. Lett. **119**, 147202 (2017).
- <sup>92</sup> F. Xu, G. Li, J. Chen, Z. Yu, L. Zhang, B. Wang, and J. Wang, Phys. Rev. B **108**, 144409 (2023).
- <sup>93</sup> B. Wang, J. Wang, and H. Guo, Phys. Rev. B **69**, 153301 (2004).
- <sup>94</sup> F. M. Souza, A. P. Jauho, and J. C. Egues, Phys. Rev. B **78**, 155303 (2008).
- <sup>95</sup> M. Filipović and W. Belzig, Phys. Rev. B **97**, 115441 (2018).
- <sup>96</sup> C. Romeike, M. R. Wegewijs, W. Hofstetter, and H. Schoeller, Phys. Rev. Lett. **96**, 196601 (2006).
- <sup>97</sup> J. J. Parks, A. R. Champagne, T. A. Costi, W. W. Shum, A. N. Pasupathy, E. Neuscamman, S. Flores-Torres, P. S. Cornaglia, A. A. Aligia, C. A. Balseiro, G. K.-L. Chan, H. D. Abruña, and D. C. Ralph, Science **328**, 1370-1373 (2010).
- <sup>98</sup> F. Elste and C. Timm, Phys. Rev. B **81**, 024421 (2010).
- <sup>99</sup> M. Misiorny, I. Weymann, and J. Barnaś, Phys. Rev. B **86**, 035417 (2012).
- <sup>100</sup> Y. Li, H. Kan, Y. Miao, S. Qiu, G. Zhang, J. Ren, C. Wang, and G. Hu, Physica E **124**, 114327 (2020).
- <sup>101</sup> R.-Q. Wang, L. Sheng, R. Shen, B. Wang, and D. Y. Xing, Phys. Rev. Lett. **105**, 057202 (2010).
- <sup>102</sup> M. Misiorny and J. Barnaś, Phys. Rev. B **89**, 235438 (2014).
- <sup>103</sup> M. Misiorny and J. Barnaś, Phys. Rev. B **91**, 155426 (2015).
- <sup>104</sup> M. Misiorny and J. Barnaś, Phys. Rev. B **76**, 054448 (2007).
- <sup>105</sup> Z. Zhang and L. Jiang, Nanotechnology **25**, 365201 (2014).
- <sup>106</sup> A. Płomińska and I. Weymann, Phys. Rev. B **94**, 035422 (2016).
- <sup>107</sup> A. Płomińska and I. Weymann, Journal of Magnetism and Magnetic Materials **480**, 11-21 (2019).
- <sup>108</sup> J. R. Petta, S. K. Slater, and D. C. Ralph, Phys. Rev. Lett. **93**, 136601 (2004).
- <sup>109</sup> U. Ham and W. Ho, Phys. Rev. Lett. **108**, 106803 (2012).
- <sup>110</sup> G. Czap, P. J. Wagner, F. Xue, L. Gu, J. Li, J. Yao, R. Wu, and W. Ho, Science **364**, 670 (2019).
- <sup>111</sup> A. Landig, J. Koski, P. Scarlino, C. Reichl, W. Wegscheider, A. Wallraff, K. Ensslin, and T. Ihn, Phys. Rev. Lett. **122**, 213601 (2019).
- <sup>112</sup> M. Urdampilleta, S. Klyatskaya, J. -P. Cleuziou, M. Ruben, and W. Wernsdorfer, Nature Mater. **10**, 502 (2011).
- <sup>113</sup> U. Ham and W. Ho, J. Chem. Phys. **138**, 074703 (2013).
- <sup>114</sup> L. Landau and E. M. Lifshitz, Phys. Z. Sowjetunion **8**, 153 (1935).
- <sup>115</sup> T. L. Gilbert, Phys. Rev. **100**, 1243 (1955).
- <sup>116</sup> T. Gilbert, IEEE Trans. Magn. **40**, 3443 (2004).
- <sup>117</sup> J. Xiao, G. E. W. Bauer, K. C. Uchida, E. Saitoh, and S. Maekawa, Phys. Rev. B **81**, 214418 (2010).
- <sup>118</sup> S. K. Kim and Y. Tserkovnyak, Phys. Rev. B **92**, 020410 (2015).
- <sup>119</sup> L. Arrachea and F. von Open, Physica E **74**, 596-602 (2015).
- <sup>120</sup> J. Fransson, Nanotechnology **19**, 285714 (2008).
- <sup>121</sup> N. Bode, L. Arrachea, G. S. Lozano, T. S. Nunner, and F. von Oppen, Phys. Rev. B **85**, 115440 (2012).
- <sup>122</sup> L. Berger, J. Appl. Phys. **3**, 2156 (1978).
- <sup>123</sup> S. Zhang and Z. Li, Phys. Rev. Lett. **93**, 127204 (2004).
- <sup>124</sup> K. M. D. Hals and A. Brataas, Phys. Rev. B **89**, 064426 (2014).
- <sup>125</sup> M. Sayad, R. Rausch, and M. Potthoff, Phys. Rev. Lett. **117**, 127201 (2016).
- <sup>126</sup> M. O. A. Ellis, M. Stamenova, and S. Sanvito, Phys. Rev. B **96**, 224410 (2017).
- <sup>127</sup> U. Bajpai and B. Nikolić, Phys. Rev. B **99**, 134409 (2019).
- <sup>128</sup> A. Suresh, U. Bajpai, and B. K. Nikolić, Phys. Rev. B **101**, 214412 (2020).
- <sup>129</sup> M. Elbracht and M. Potthoff, Phys. Rev. B **102**, 115434 (2020).
- <sup>130</sup> R. Smorka, M. Thoss, and M. Žonda, New. J. Phys. **26**, 013056 (2024).
- <sup>131</sup> M. Filipović, arXiv:2408.02823 (2024).
- <sup>132</sup> G. Floquet, Ann. Sci. Ecole Normale Supérieure **12**, 47 (1883).
- <sup>133</sup> Jon H. Shirley, PhD Thesis, California Institute of Technology, (1963).
- <sup>134</sup> M. Grifoni and P. Hänggi, Phys. Rep. **304**, 229 (1998).
- <sup>135</sup> B. H. Wu and C. Timm, Phys. Rev. B **81**, 075309 (2010).
- <sup>136</sup> C. Kittel, Phys. Rev. **73**, 155 (1948).
- <sup>137</sup> B. Wang, J. Wang, and H. Guo, Phys. Rev. B **67**, 092408 (2003).
- <sup>138</sup> H. Bruus and K. Flensberg, *Many-Body Quantum Theory in Condensed Matter Physics* (Oxford University Press, Oxford, UK, 2004).
- <sup>139</sup> Y. M. Blanter and M. Büttiker, Phys. Rep. **336**, 1 (2000).
- <sup>140</sup> A. Fetter and J. D. Walecka, *Quantum Theory of Many-Particle Systems* (Dover, Mineola, NY, 2003).
- <sup>141</sup> D. C. Langreth, in *Linear and Nonlinear Electron Transport in Solids*, edited by J. T. Devreese and E. Van Doren (Plenum, New York, 1976).
- <sup>142</sup> U. Fano, Phys. Rev. **124**, 1866 (1961).
- <sup>143</sup> A. E. Miroschnichenko, S. Flach, and Y. S.

Kivshar, Rev. Mod. Phys. **82**, 2257 (2010).